Pergamon

Geochimica et Cosmochimica Acta, Vol. 66, No. 1, pp. 125–143, 2002

0016-7037/02 $22.00 + .00

PII S0016-7037(01)00736-0

Empirical models relating viscosity and tracer diffusion in magmatic silicate melts

JAMES E. MUNGALL*
Department of Geology, University of Toronto, 22 Russell St., Toronto, ON M5S 3B1, Canada

(*Received June* 28, 2000; *accepted in revised form January* 4, 2001)

Abstract—The Adam-Gibbs equations describing relaxation in silicate melts are applied to diffusion of trace components of multicomponent liquids. The Adam-Gibbs theory is used as a starting point to derive an explicit relation between viscosity and diffusion including non-Arrhenian temperature dependence. The general form of the equation is $D_i\eta = A_i\exp\{\Delta(s_cE_i)/TS_c\}$, where D is diffusivity, η is melt viscosity, T is absolute temperature, $\Delta(s_cE_i)$ is the difference between the products of activation energies and local configurational entropies for viscous and diffusive relaxation, A_i is a constant that depends on the characteristics of the diffusing solute particles, and S_c is configurational entropy of the melt. The general equation will be impractical for most predictive purposes due to the paucity of configurational entropy data for silicate melts. Under most magmatic conditions the proposed non-Arrhenian behaviour can be neglected, allowing the general equation to be simplified to a generalized form of the Eyring equation to describe diffusion of solutes that interact weakly with the melt structure: $D_i\eta/T = Q_i\exp\{\Delta E_i/RT\}$, where Q_i and ΔE_i depend on the characteristics of the solute and the melt structure. If the diffusing solute interacts strongly with the melt structure or is a network-forming cation itself, then $\Delta E_i = 0$, and the relation between viscosity and diffusion has the functional form of the classic Eyring and Stokes-Einstein equations; $D_i\eta/T = Q_i$. If the diffusing solute can make diffusive jumps without requiring cooperative rearrangement of the melt structure, the diffusivity is entirely decoupled from melt viscosity and should be Arrhenian, i.e., $D_i = Q_i\exp\{B_i/T\}$. A dataset of 594 published diffusivities in melts ranging from the system CAS through diopside, basalt, andesite, anhydrous rhyolite, hydrous rhyolite, and peralkaline rhyolite to albite, orthoclase, and jadeite is compared with the model equations. Alkali diffusion is completely decoupled from melt viscosity but is related to melt structure. Network-modifying cations with field strength Z_i^2/r between 1 and 10 interact weakly with the melt network and can be modelled with the extended form of the Eyring equation. Diffusivities of cations with high field strength have activation energies essentially equal to that of viscous flow and can be modelled with a simple reciprocal Eyring-type dependence on viscosity. The values of Q_i, ΔE_i and B_i for each cation are different and can be related to the cation charge and radius as well as the composition of the melt through the parameters Z_i^2/r, M/O, and Al/(Na + K + H). I present empirical fit parameters to the model equations that permit prediction of cation diffusivities given only charge and radius of the cation and temperature, composition and viscosity of the melt, for the entire range of temperatures accessible to magmas near to or above their liquidus, for magmas ranging in composition from basalt through andesite to hydrous or anhydrous rhyolite. Pressure effects are implicitly accounted for by corrections to melt viscosity. Ninety percent of diffusivities predicted by the models are within 0.6 log units of the measured values.

1. INTRODUCTION

When a geochemical system is perturbed it will tend to return to an equilibrium state by the transfer of chemical components between coexisting phases. The mechanism by which mass transfer takes place is the irreversible thermodynamic process of chemical diffusion (Ghiorso, 1987). A quantitative description of a dynamic magmatic system thus depends on the availability of activity-composition models for all phases present, and upon the estimation of diffusion coefficients for all components of interest in the melt phase.

Many people have investigated chemical and tracer diffusion in silicate melts, and there are well over 1000 published diffusion coefficients of cations in natural or analog silicate melts. Reviews of this sizable data set have revealed extreme variability in observed rates of diffusion while hinting at the existence of underlying order in the sum of the available data (Hofmann, 1980; Jambon, 1982; Henderson et al., 1985; Dingwell, 1990; Chakraborty, 1995). Considering the fundamental identity of diffusion and viscous flow (Glasstone et al., 1941), and the remarkable success of simple empirical models in predicting viscosities of silicate liquids over very wide ranges of compositions and temperatures (Bottinga and Weill, 1972; Shaw, 1972; Hess and Dingwell, 1995), it is perhaps surprising that a successful general relation between viscosity and diffusion has never been established.

In this communication I extend previous theoretical descriptions of viscous flow and diffusion to arrive at equations that relate these two processes in a very general way. I then compare all the available published diffusion coefficients for cations in geologically relevant silicate melts with the model equations. There are very few examples of published diffusivities that do not fit into one of three simple empirical expressions based on the model equations, within a margin of error of about one half log unit.

2. THEORY

2.1. Tracer Diffusion

This article is concerned with tracer diffusivity; it is important to distinguish between different types of diffusion coeffi-

* (mungall@geology.utoronto.ca).

cient. In the case of self diffusion, there is no change in chemical potential of solute species throughout the diffusion region. This condition can be approximated by experimental determinations of tracer diffusivity, by introducing a different isotopic mixture of the species in question to a portion of a system while ensuring that the bulk chemical composition is constant throughout. To the extent that different isotopes of a chemical element can be assumed to have identical mobilities, tracer diffusivities approximate well to self-diffusivities, which describe the mobility by random walk of individual solute particles in the absence of any driving force. As has been elegantly documented by Richter et al. (1999), the tracer diffusivity of an individual isotope may vary significantly from that of the chemical element as whole.

The diffusion coefficient of a solute species that is subject to gradients either of its own chemical potential or those of other species present is a chemical diffusion coefficient. In the case of binary chemical diffusion there is a chemical potential gradient, but interdiffusion of the two melt components can be described by a single diffusion coefficient. In all situations not covered by the special cases of tracer diffusion or binary chemical diffusion the flux will depend on the concentration gradients of other melt components in a complex way. The full description of such multicomponent effects can be found elsewhere (e.g., Kuiken, 1994).

Chemical diffusion coefficients of a single component in a geologic melt have been observed to vary by several orders of magnitude even in a single melt composition at a single temperature, depending on the magnitude of the fluxes of other species present (Mungall et al., 1998). The chemical diffusion coefficients of solutes present at trace abundances in systems not characterized by large gradients in the concentrations of other species may be very similar to true tracer diffusivities. A more extensive discussion of the justification for this statement was given by Mungall et al. (1999). For the remainder of this article I will equate chemical and tracer diffusivities, excluding from the discussion any case in which the chemical diffusivities were likely to have been affected by multicomponent effects.

Tracer diffusivities are directly applicable to mass transfer problems in natural systems where large gradients in the major element concentrations are absent. One prime example of this is the partitioning of very strongly compatible or highly incompatible elements between pairs of phases, including silicate melt–sulphide melt pairs, silicate melts and incompatible element–rich crystals such as zircon, or silicate melts and incompatible element–poor crystals such as feldspar in feldspar-rich melts. Another example of an application of tracer diffusion is the homogenization of radiogenic isotope ratios during magma mixing (e.g., Lesher 1990, 1994). It may also be possible in the future to constrain chemical diffusivities through the application of models relating tracer and chemical diffusivities if a method of estimation of the tracer diffusivities is already available (e.g., Liang et al., 1997).

2.2. Viscosity and Diffusion

It has been recognized for a very long time that the processes allowing stress relaxation by viscous flow in melts are identical at some level with diffusive motion, and that it should therefore be possible to find quantitative links between the rates of the two processes. In the Appendix, I present a brief summary of past attempts to link these two processes and introduce a new approach based on the Adam-Gibbs equations.

The form of the classic Eyring equation (Eqn. A3) is identical to that of the Stokes-Einstein equation (Eqn. A1), despite the profound differences in their derivation, and can be represented by the functional form

$$\frac{D_i\eta}{T} = Q_i, \tag{1}$$

where Q_i is a constant for each diffusing component in a given melt that can in principle be related to real physical quantities by comparison with Eqn. A3; that is, for the case of the Eyring equation,

$$Q_i = \frac{\kappa}{\lambda_i}. \tag{2}$$

All parameters used in these and following equations are defined in the Appendix.

The Eyring equation can be used with great success to relate the diffusion of high–field strength network-forming cations and oxygen to the viscosity of a silicate melt (e.g., Chakraborty et al., 1995; LaTourette et al., 1996; Lesher et al., 1996; Liang et al., 1996; Mungall and Dingwell, 1997).

Despite its success in some instances, Eqn. 1 commonly fails (Hofmann, 1980). The form of Eqn. A2 offers the novel advantage over both the Eyring and Stokes-Einstein equations of offering the possibility of a difference in activation energy between diffusive and viscous mass transfer, while retaining a fundamental link between the two processes. Such behaviour was described by Mungall et al. (1999), who showed that the difference between the activation energy of diffusion and that of viscous flow remained similar in granitoid melts at a wide variety of melt viscosities, causing cation diffusivities to migrate in concert around an Arrhenius plot as viscosity was varied by changing the melt composition.

If the mechanisms of diffusive motion for particular ions do not change much with temperature or melt composition, then λ_i, m_i, and ν_i in Eqn. A2 will be constants. Similarly, λ_ν, m_ν, and ν_ν may be constant over large ranges in viscosity. With these assumptions the unknown terms and κ in Eqn. A2 can be collected into a single constant Q_i for each ion. Converting to molar quantities gives the following relation:

$$\frac{D_i\eta}{T} = Q_i \exp\left\{\frac{\Delta E_i}{RT}\right\}, \tag{3}$$

where R is the ideal gas constant and ΔE_i expresses the difference between the activation energy for diffusive motion of a particular ion and the activation energy for viscous rearrangement of the melt structure–forming ions. The constant Q_i now contains information about particle sizes, masses, and the degree of constriction of their local atomic environment as represented by the free volume

$$Q_i = \frac{\lambda_i^2\kappa}{\lambda_\nu^3}\left(\frac{\nu_\nu}{\nu_i}\right)^{1/3}\left(\frac{m_\nu}{m_i}\right)^{1/2}. \tag{4}$$

The Adam-Gibbs approach to describing viscous flow and diffusion given by Eqn. A6 can be expressed in the general form

$$D_i\eta = Q_i \exp\left\{\frac{\Delta(s_c E_i)}{RTS_c}\right\}, \quad (5)$$

where the constant Q_i again contains information about both the particle and general melt properties. Eqn. 5 is relevant to the diffusion of solute particles whose motion requires cooperative rearrangements of the melt structure.

Solute particles whose motion might involve some part of the melt structure in the formation of their activated complex for diffusion, but does not result in any net change in the network-forming melt structure that controls viscous stress relaxation, will show diffusivities uncoupled from viscosity as shown in the generalized form of Eqn. A7;

$$D_i = Q_i \exp\left\{\frac{B_i}{RT}\right\}, \quad (6)$$

where Q_i and B_i again contain information about the characteristics of both solute and melt, and will therefore depend upon melt composition and the solute type.

The application of the Adam-Gibbs formalism to describe diffusion in melts is general, and has sufficient flexibility to describe a wide variety of diffusive behaviours. The minor temperature dependence shown by the left-hand side of Eqn. 3 was neglected in the derivation of Eqn. A6 so that the only substantive difference between Eqn. 3 and 5 resides in the configurational entropy terms, despite the fact that the two equations were derived from entirely different physical arguments and the nominal identity of the constants Q_i in each of the two differs considerably. Configurational entropy exerts a strong control upon viscosity over the temperature range from liquidus to glass transition for many melts relevant to geology. However, because most silicate melts exist at or near their liquidus under normal circumstances, non-Arrhenian behaviour resulting from temperature dependent changes in configurational entropy will not be evident under normal circumstances. The obvious exception to this generality is the formation of glassy rocks during volcanic processes accompanied by extreme undercooling. Leaving aside the cases in which the temperature dependence of configurational entropy is important, Eqn. 5 can be simplified to the form of Eqn. 3 by holding S_c constant.

The difference between Eqn. 1 and 3 consists in the presence of a difference between the activation energy of diffusion and that of viscosity. If the difference in activation energy is zero, then Eqn. 3 becomes identical to Eqn. 1.

Although non-Arrhenian diffusion is rarely reported in silicate melts, it is commonly displayed near to the glass transition (e.g., Caillot et al., 1994; Kincs and Martin, 1996) by highly mobile cations. Non-Arrhenian diffusion of relatively immobile elements would be difficult to observe, because of the inordinate amounts of time required to generate measurable diffusion profiles at temperatures near to the glass transition temperature for species whose diffusivity is subequal to that of the network-forming cations that control viscosity.

In summary, the Adam-Gibbs equations can be manipulated to derive a series of equations describing various types of diffusive behaviour in relation to the viscosity of the enclosing melt. Progressive introduction of simplifying assumptions allows the general equation to be reduced to two variants of the Eyring equation (Eqn. 1 and 3) showing explicit relations between viscosity and diffusion, or to a third version (Eqn. 6) that describes diffusion that is entirely decoupled from the motions of the melt structure that permit viscous flow.

3. DATA

I have compiled over 1000 published measurements of diffusion coefficients for cations in silicate melts of natural or analog compositions corresponding to a range from basalt through rhyolite. After screening the data as detailed below, I am left with 594 usable diffusivities. The data have been generated in a number of ways, and vary considerably in their reliability. It is beyond the scope of this article to review the methods by which diffusion coefficients may be measured, and the interested reader should consult the original data sources. All data available were included subject to the following restrictions: Published values must have been measured in melts whose viscosity is known or can be calculated. Data collected below the glass transition temperature are excluded, and data for elements suspected to exist simultaneously in multiple oxidation states were not included in the fitting procedure. The contents of the data set are too large to be presented here, but the coverage and sources are outlined in Table 1. Also listed in Table 1 are the sources of the models used to constrain the viscosities of the melts in which the diffusivities were measured.

An important parameter in the models described below is cation radius. I have used ionic radii published by Shannon (1976) for reasonable and convenient choices of coordination number. Most cation radii are for octahedral coordination, with the following exceptions: Be is assumed to be in trigonal coordination whereas Si, Al, and Ge are assumed to be in tetrahedral coordination. Although some of my choices for coordination number are probably wrong, the resulting variation in cation field strength does not propagate into significant errors in estimated diffusion coefficients, because the dependences of field strength on radius tend to be rather weak. The main exceptions to this generalization are the alkalis. Whatever the true coordination numbers might be, the current model is calibrated assuming octahedral coordination for alkali cations and therefore if it is to be extrapolated to other species the user should also assign octahedral coordination in the estimation of cation radius.

It is impossible to fit the equations to the entire data set. A small number of published data are clearly outliers, in most cases showing diffusivities too high to be accounted for by the model equations. Outliers were rejected only in those cases where other data for ions with similar charge and radius in similar or identical melt compositions showed radically different rates of diffusion. The rejected data are derived from only three studies. To preserve continuity in the following discussion I will describe all of the rejected outliers here, before I begin to present the results of the fitting exercise.

One set of data represents early measurements of ^{45}Ca tracer diffusion profiles using β track analysis (Watson 1979, 1981). At the time when these studies were carried out it was thought

Table 1. Sources of data and viscosity models.

Reference	Melt composition	Method of viscosity calculation	Elements
1. Jambon and Carron (1976)	albite	n.a.	Na, K, Rb, Cs
	orthoclase	n.a.	Na, K, Rb, Cs
2. Hofmann and Magaritz (1977)	basalt	Shaw (1972)	Ca, Sr, Ba, Co
3. Jambon and Semet (1978)	obsidian	n.a.	Li
	albite	n.a.	Li
	orthoclase	n.a.	Li
4. Magaritz and Hofmann (1978)	obsidian	Shaw (1972)	Sr, Ba, Na
5. Watson (1981)	obsidian LCO	Hess and Dingwell (1996)	Na, Cs, Ca
	LCO + H_2O	Hess and Dingwell (1996)	Na, Cs, Ca
6. Lowry et al. (1982)	basalt	Shaw (1972)	Co, Mn, Sr, Ba, Na, Cs, Sc, Eu
	andesite	Shaw (1972)	Co, Mn, Sr, Ba, Na, Cs, Sc, Eu
7. Jambon (1982)	obsidian OIS	Hess and Dingwell (1996)	Cs, Na, K, Rb, Ca, Ba
	obsidian OVD	Hess and Dingwell (1996)	Cs, Eu, Ce
8. Harrison and Watson (1983)	obsidian + H_2O	Hess and Dingwell (1996)	Zr
9. Henderson et al. (1985)	pitchstone	Shaw (1972)	Ba, Cs, Co, Fe, Mn, Na, Eu
	pantellerite	Shaw (1972)	Ba, Cs, Co, Fe, Mn, Na, Eu
	basalt	Shaw (1972)	Eu
	andesite	Shaw (1972)	Eu
10. Shimizu and Kushiro (1991)	jadeite-diopside join	Shaw (1972)	Mg, Ca, Si
11. Behrens (1992)	anorthite-albite join	Hummel and Arndt (1985)	Na, Ca
12. Baker (1992b)	dacite	Shaw (1972)	Si, B, Ga
	obsidian LCO	Hess and Dingwell (1996)	Si, B, Ga
13. LaTourette et al. (1996)	haplobasalt	Shaw (1972)	Mg, Ca, Ba, Nd, Yb, Ti, Zr, U
14. Lesher et al. (1996)	basalt	Shaw (1972)	Si
15. Liang et al. (1996)	Ca-Al-Si-O system	Shaw (1972)	Ca, Al, Si
16. Mungall and Dingwell (1997)	haplogranite	Hess and Dingwell (1996)	U, Th
	haplogranite + H_2O	Hess and Dingwell (1996)	U, Th
17. Roselieb and Jambon (1997)	jadeite	Richet (1984)	K, Rb, Cs
18. Nakamura and Kushiro (1998)	jadeite	Richet (1984), Kushiro (1976)	La, Ce, Pr, Nd, Sm, Eu, Gd, Dy, Er, Yb, Lu, Ba, Sr, Rb, Y, Zr, Nb, Th, U
	diopside	Richet (1984), Scarfe et al. (1979)	La, Ce, Pr, Nd, Sm, Eu, Gd, Dy, Er, Yb, Lu, Ba, Sr, Rb, Ba, Sr, Rb
19. Mungall et al. (1999)	haplogranite	measured	Cs, Be, Mg, Ca, Sr, Ba, B, Y, Nd, Tb, Lu, Ti, Zr, Ge, Nb, Hf, Ta, W
	haplogranite + H_2O	Hess and Dingwell (1996)	Cs, Be, Mg, Ca, Sr, Ba, B, Y, Nd, Tb, Lu, Ti, Zr, Ge, Nb, Hf, Ta
	haplogranite + Na_2O	measured	Cs, Be, Mg, Ca, Sr, Ba, B, Y, Nd, Tb, Lu, Ti, Zr, Ge, Nb, Hf, Ta, W

that β particle penetration distances in glass were on the order of 1 to 10 μm (Mysen and Seitz, 1974). It has since been discovered that the β particle penetration distances in geological materials are some 2 orders of magnitude greater than was thought in 1981 (Tingle, 1987). Using currently available β ranges (International Commission on Radiation Units and Measurements, 1984) the maximum distance of travel in silicate glass for β particles derived from decay of ^{45}Ca can be estimated as approximately 330 μm. Deconvolution of the effects of β penetration from the actual diffusion profiles (Ganguly et al., 1988) indicates that a ^{45}Ca profile 1.2 mm long will provide an estimate of D^{Ca} about twice the true value. Shorter profiles will show much greater errors with magnitudes that cannot be calculated reliably. Indeed, many of the diffusion coefficients presented by Watson in these two early papers (Watson, 1979, 1981) are much larger than corresponding data measured in similar materials by other methods. In light of these uncertainties I have chosen to exclude from my fitting procedure all of the diffusivities measured by β track methods.

A second set of values that differ significantly and systematically from all other similar published diffusion coefficients are the chemical diffusion coefficients of Ga measured in dacite and rhyolite melt using a thin-source configuration by Baker (1992b). Aspects of the experimental approach make it difficult to compare the measured diffusion coefficients with other published data. The thin sources of Ga in these experiments were dilute aqueous solutions of $GaCl_3$ dried onto the ends of polished rhyolite glass cylinders. The diffusivities of B measured in this way in the same study are in excellent agreement with other data in my compilation, but the reported Ga diffusivities are consistently at least an order of magnitude larger than expected. I cannot account for this discrepancy except to suggest that the Ga was deposited on the glass cylinders as a hydroxide species that then contributed a nontrivial amount of water (1.5 mol H_2O for each mole of Ga) to the rhyolite melt during the diffusion anneal at high temperature and pressure. The amount of water this would add to the melt in the diffusion region can be estimated at between 1.0 and 0%, leading to an unconstrained reduction in the melt viscosity of up to 1 order of magnitude over the length of the Ga diffusion profiles. The predicted decrease of viscosity agrees qualitatively with the observation that Ga diffusion coefficients measured were about 1 order of magnitude greater than expected in the context of the present model, and mirrors other observations of radical increases in

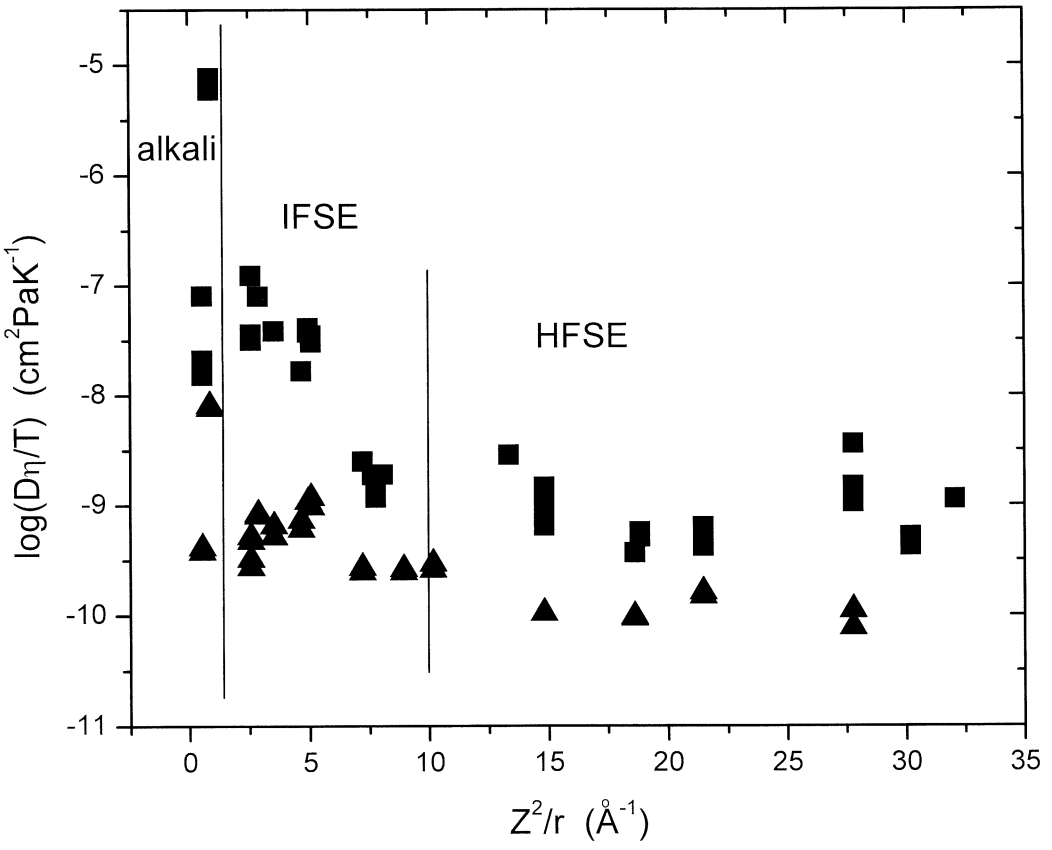

Fig. 1. Log($D_i\eta/T$) vs Z_i^2/r for selected data measured at 1400 °C. Symbols: squares – values measured in rhyolite melts; triangles – values measured in basaltic melts. Data sources: references 6, 13, 16, 19 in Table 1.

diffusion coefficients of high–field strength cations upon the addition of small amounts of depolymerizing agents to highly polymerized rhyolitic melts (Mungall and Dingwell, 1997).

The thin source used in the same study (Baker, 1992b) to measure ^{30}Si tracer diffusion coefficients was a layer up to 100 μm thick of glass powder doped with ^{30}Si and having the approximate composition $(Na_2O)_{0.27}(SiO_2)_{0.73}$. This powder layer was placed against the end of the rhyolite glass and the resulting couple was annealed. ^{30}Si profiles were measured by ion probe and the diffusion coefficient was estimated using a thin-source model on profiles ranging from 50 to 400 μm in length. The initial configuration was thus an extended source with a thickness in some cases as long as the length of the final profile, invalidating the use of the thin-source model for data reduction. Furthermore, the composition of the extended source of ^{30}Si was very different from that of the melt in which the diffusion coefficient was ostensibly being measured. The experimental configuration was therefore that of a chemical diffusion couple, finite on one side and infinite on the other, with large variations in melt composition and viscosity throughout the interface region where diffusion was taking place. I have therefore not included these data in the fit, although some of them do fall quite close to the rest of the data.

Chemical diffusivities of B measured in the same study (Baker, 1992b) were not subject to the same kinds of uncertainty and have been included in the fitting procedure below.

Colson et al. (1995) presented a large number of diffusion coefficients for Ni in synthetic melts with compositions analogous to basalts. The study was aimed primarily at inferring activity-composition relations and the diffusion coefficients were measured relatively indirectly by an electrochemical method on melt drops with poorly controlled geometry. The resulting data set shows a great deal of scatter with a centroid quite near to the values expected in the present context. I have accordingly omitted these data from the fitting procedure.

Finally, a small number of the diffusion coefficients recently presented by Mungall et al. (1999) differ from expected values by up to 1 order of magnitude; this is not surprising considering the relatively low precision of the electron microprobe measurements used to constrain the diffusivities. The errant points represent only ~3% of the sum of data presented in that study, the rest of which conforms well to expected values. I have consequently retained all of the data from Mungall et al. (1999) on the grounds that I cannot justify omitting one or two points simply because they do not fit the model.

4. PREDICTIVE EMPIRICAL MODELS

4.1. Previous Work

Numerous workers have applied the classic form of the Eyring equation to tracer diffusion in silicate melts (for some examples see references in Hofmann, 1980; Dingwell, 1990; Chakraborty, 1995; LaTourette et al., 1996; Mungall and Ding-

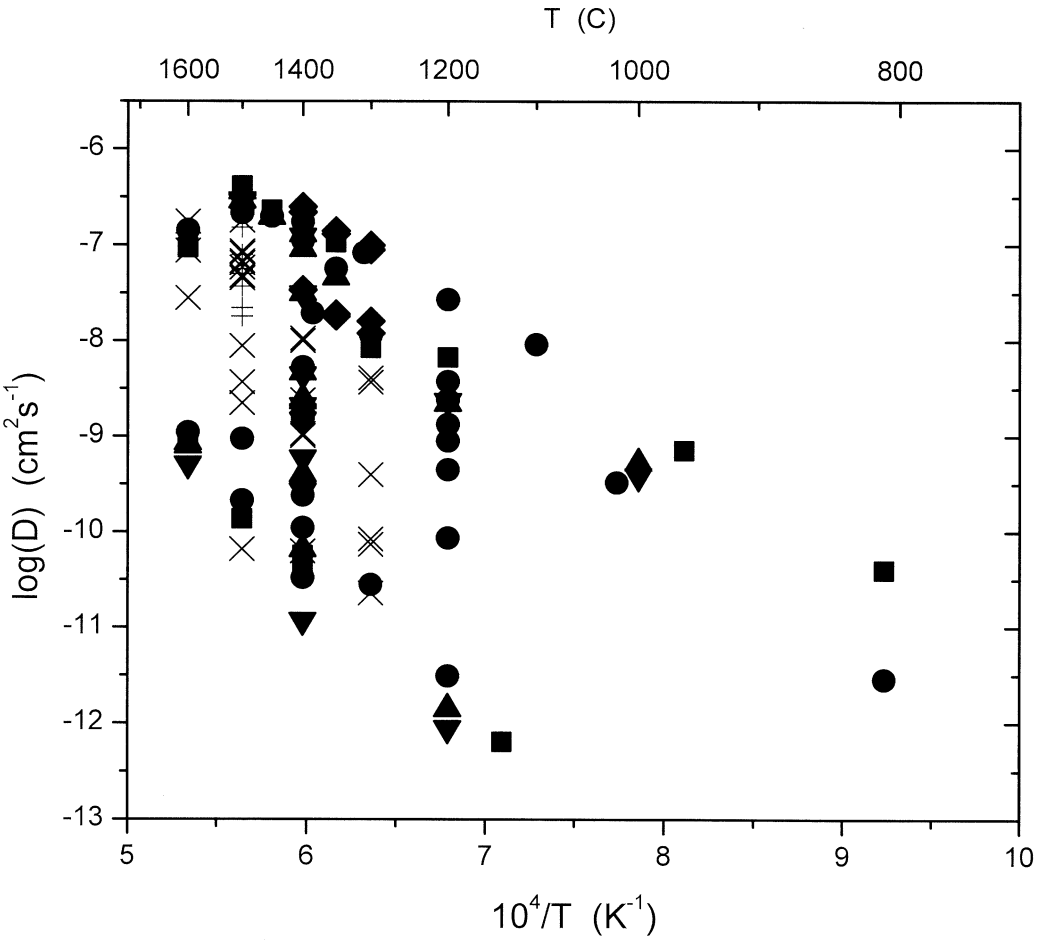

Fig. 2. Log(D_i) vs $10^4/T$ for selected HFSE data. Symbols: Squares – Ti; circles – Zr; up triangles – U; down triangles – Th; diamonds – Sc; cross – Al; x – Si. Data sources: references 6, 8, 13, 15, 18, 19 in Table 1.

well, 1997; Mungall et al., 1999). The consensus has been that the Eyring equation works well for network-forming ions but not others. Jambon (1982) compiled existing data for anhydrous rhyolites and established a model relating diffusion to cation charge and radius. Jambon (1982) argued against a significant role for melt composition in controlling diffusion; however, his database included a restricted number of melt compositions and elements.

Baker (1990, 1992a) successfully applied Eyring's treatment of viscosity and diffusion to network-former and alkali diffusion in albite melts. In the absence of detailed knowledge of the atomic scale mechanisms of diffusive motion and associated viscous flow, it was necessary to make simple assumptions for quantities such as the mass of diffusing particles and the free volume of individual species. Baker used the heat of vaporization of Na_2O melt to estimate the free volume and activation energy for Na, and the heat of vaporization of albite melt to estimate the free volume and activation energy for network-forming ions. Although heats of vaporization worked in the case of albite, the activation energy for Na diffusion varies greatly with melt composition (see Section 4.5), whereas the heat of vaporization of Na_2O can give only one estimate of activation energy. As a result of such uncertainty, this type of approach is necessarily ad hoc and currently impossible to extend to predictive models with wide application.

4.2. Model Equations

The principal aim of this paper is to provide a set of empirical models for diffusion that will allow one to predict the diffusivity of an arbitrarily chosen cation in any geological melt at any temperature. This is accomplished by comparing published data with Eqn. 3 or 6. Since the parameters Q_i, B_i, and ΔE_i may be different for each element, and may also differ from one melt composition to another, it is necessary to make each of these parameters itself a function of cation characteristics and of melt composition. Considering the variety of ways in which simple relations such as Eqn. 1 can be derived (see discussion in the Appendix and the preceding section), attempts to find genuine physical significance in the parameter Q_i appear to be of rather dubious value. Whereas the derivations of the Eyring and Stokes-Einstein equations posit firm but contradictory meanings for these constants, Adam and Gibbs (1965) declined to specify the physical significance of their corresponding preexponential term A_i.

All of the species considered here are electrically charged

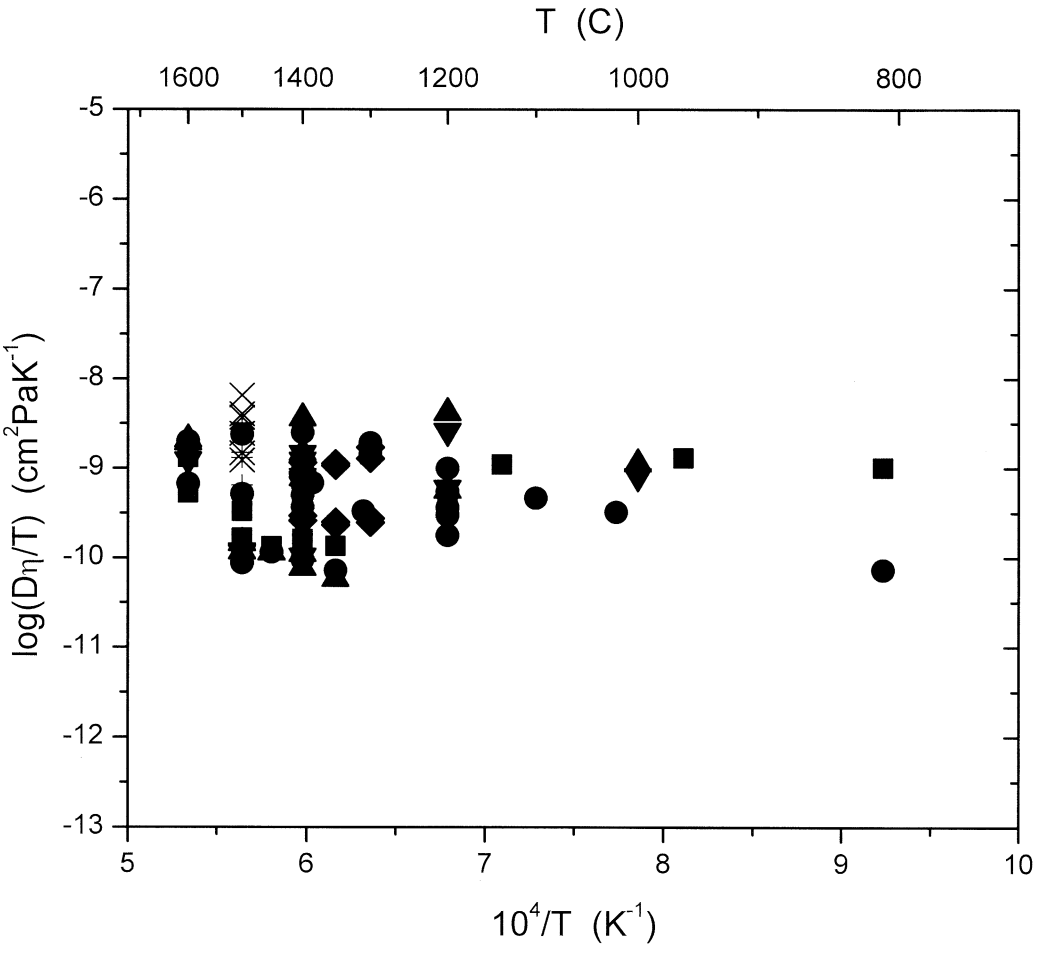

Fig. 3. Log($D_i\eta/T$) vs $10^4/T$ for selected HFSE data. Symbols as in Figure 2. Note that almost all of the variation in diffusivity is eliminated by normalizing to viscosity. Data sources: references 6, 8, 13, 15, 18, 19 in Table 1.

and therefore their mobility is expected to be largely controlled by coulombic forces, which are not explicitly included in the model equations. The role of ionic charge can be encapsulated in the parameter Z_i^2/r, or field strength, which relates charge Z_i to radius r of each species. The compositional parameters used are M/O (Henderson et al., 1985), which relates the molar proportion of network-modifying cations M to the molar proportion of oxygen ions O in the melt; and the molar ratio Al/(Na + K + H), which relates to the proportion of alkali cations not bound to tetrahedrally coordinated Al in a local charge-balancing role.

The choice of model equations is made on the basis of the observed variation of log($D_i\eta/T$) with field strength Z_i^2/r, shown in Figure 1. The data shown in Figure 1 were all measured at 1400°C, so that the effects of temperature are not evident. The quantity log($D_i\eta/T$) varies through 5 orders of magnitude for the data shown, indicating that Eqn. 1 or 3 alone cannot account for the data. Two controls on log($D_i\eta/T$) can be inferred from Figure 1. First, the data for each type of melt can be broken down into three ranges of Z_i^2/r, within each of which log($D_i\eta/T$) shows a systematic variation with field strength. The ranges are separated by vertical bars in Figure 1. Over the range $0 < Z_i^2/r < 1$, corresponding to the low–field strength cations that here are all alkali cations, the quantity log($D_i\eta/T$) increases sharply with increasing field strength. In the range $1 < Z_i^2/r < 10$, the intermediate–field strength elements (IFSE), log($D_i\eta/T$) decreases fairly consistently. At values of $Z_i^2/r > 10$, corresponding to the high–field strength elements (HFSE), there is considerable scatter but log($D_i\eta/T$) is essentially constant. Second, log($D_i\eta/T$) in rhyolitic melts shows a clear overall increase above basaltic melts, implying a compositional control. The strength of the dependence of log($D_i\eta/T$) on Z_i^2/r also increases from basalt to rhyolite, indicating that the compositional effect is exerted upon both Q_i and ΔE_i.

In the following sections the three ranges of Z_i^2/r are each treated separately, taking appropriate choices of the model equations and fitting the adjustable parameters to the observed compositional and cation-specific controls. The need to treat the three ranges of field strength separately implies that sharp transitions in diffusive behaviour are encountered at field strengths of ~1 and ~10.

Goodness of fit is difficult to assess because the errors associated with the data are extremely variable and often impossible to quantify. I have chosen the χ^2 merit function, making the assumption that the errors on the published data set (i.e., log[D_i]) are normally distributed with a standard deviation

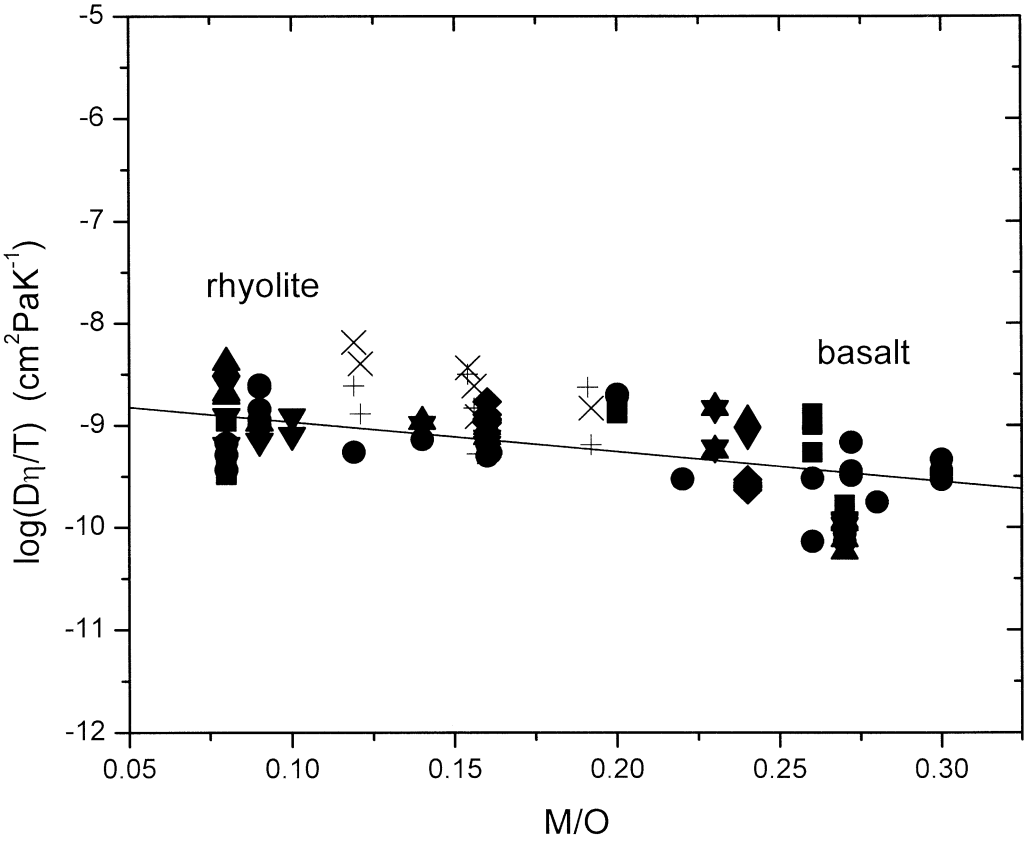

Fig. 4. Log($D_i\eta/T$) vs M/O for selected HFSE data. Symbols as in Figure 2. The subhorizontal line indicates the model trend's weak dependance on degree of melt polymerization. Data sources: references 6, 8, 13, 15, 18, 19 in Table 1.

of 0.3 log unit for all data points. If the data actually have larger standard deviations, I should calculate a smaller χ^2, giving the impression of a better fit, whereas if the data are more precise than I have assumed, the χ^2 statistic should be larger. Since many of the viscosities estimated in this study are probably accurate to within only ~0.25 log unit, and diffusivities may have large associated errors as well, the χ^2 statistics I report here should be considered to be upper bounds; that is, the fit is probably better than is implied by my χ^2 statistic. A χ^2 value less than or equal to 1 is considered to be evidence that the model successfully accounts for the variation of the data (e.g., Press et al., 1992).

4.3. HFSE

The diffusion coefficients of selected HFSE are plotted against reciprocal temperature in Figure 2. Symbols classify the data by element, as outlined in the figure caption. Log(D_i) varies through up to 6 orders of magnitude for individual species and does not show a straightforward dependence on temperature (see data for Zr, for example). In Figure 3 the same data are presented in a plot of log($D_i\eta/T$) vs. reciprocal temperature. This diagram shows that the majority of the variation expressed in Figure 2 is removed when diffusivity is divided by viscosity; that is, there is no temperature dependence outside of that implicit in the dependence of D_i on viscosity. This observation is consistent only with the application of an equation with the form of Eqn. 1, where viscosity is the primary control on D_i. The quantity log($D_i\eta/T$) still shows a variation of ~1.5 log units for individual elements, and one has already seen from Figure 1 that log($D_i\eta/T$) for the HFSE does not depend systematically on Z_i^2/r.

In Figure 4 I have plotted log($D_i\eta/T$) vs. M/O for all the data shown in the previous two figures. A gentle slope is evident in the data, indicating that most of the variation observed between basaltic and rhyolitic melts in Figure 1 (about 1 log unit) can be accounted for by the change in M/O from ~0.1 for rhyolite to ~0.3 for basalt. I have therefore fit the following equation to all the HFSE data:

$$\log \frac{D_i\eta}{T} = -8.7 - 2.87(\mathrm{M/O});\ \chi^2 = 0.55. \qquad (7)$$

Units for Eqn. 7 are cm^2s^{-1} for D_i, Pa for η, and K for T. The logarithms of diffusion coefficients estimated using Eqn. 7 are compared with the actual measurements for HFSE in Figure 5 for all the data available (n = 156). Ninety percent of points plot within 0.6 log units (i.e., 2 standard deviations) of the diagonal line along which model and measured diffusivities are equal.

Eqn. 7 can be used to provide an order-of-magnitude estimate of the diffusion coefficient of any HFSE in any silicate melt at any temperature; however, it is important to recognize

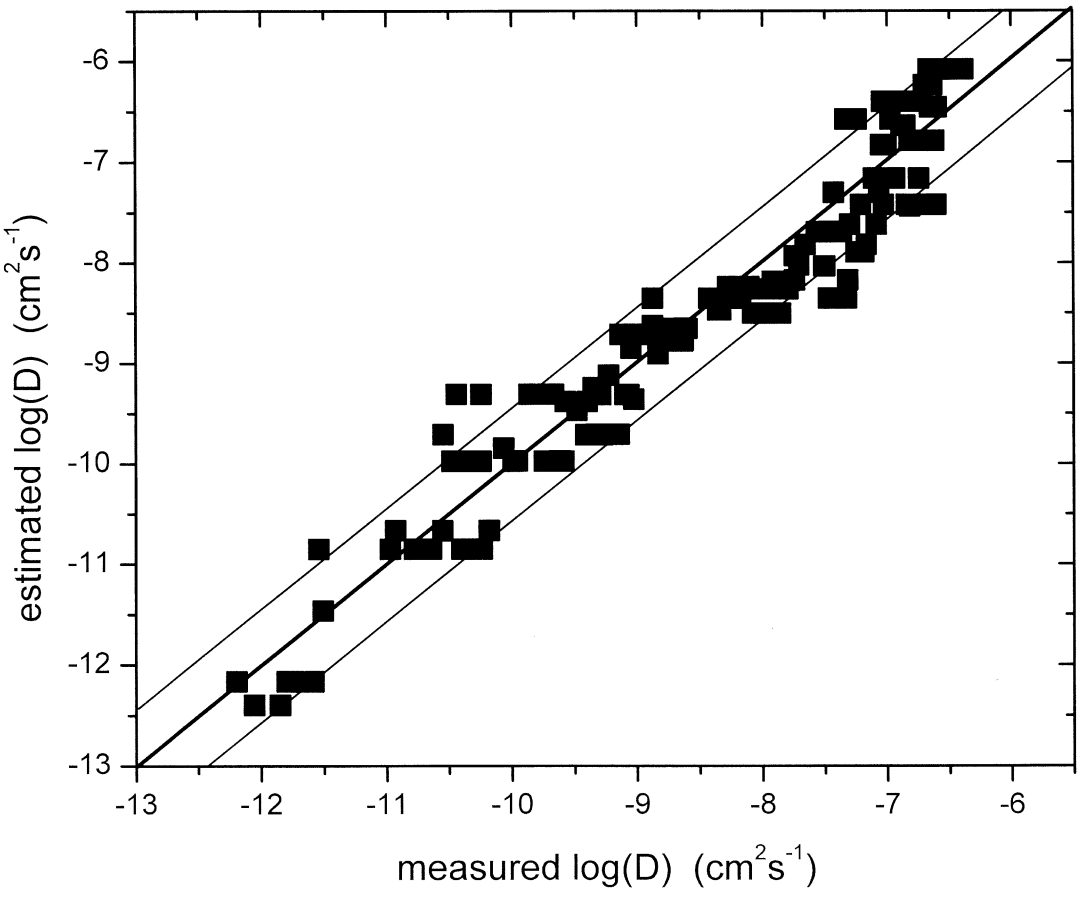

Fig. 5. Comparison of measured and estimated HFSE diffusivities. All available data are shown (references 6, 8, 10, 12, 13, 14, 15, 16, 18, 19). The bold diagonal line indicates equivalence of measurement and model. The fine diagonal lines span the range of the model plus or minus 0.6 log units (two standard deviations).

that the model predicts the same diffusivity for all HFSE in a given melt at a given temperature. This is in spite of the obvious interelement variation displayed in Figure 4. For example, all of the data for Al are displaced ~0.3 log units below the data for Si in the same melt compositions in Figure 4. This kind of fine-scale variation is lost in the model, because I have been unable to find a cation-specific parameter that accounts for it.

4.4. IFSE

The values of $\log(D_i\eta/T)$ are plotted against field strength over the range $1 < Z_i^2/r < 10$ in Figure 6 for selected isothermal data sets from two different melt compositions. At a given temperature in a given melt composition, there is a strong linear correlation between $\log(D_i\eta/T)$ and Z_i^2/r. The slope and intercept of this line vary with temperature, an observation that cannot be reconciled with Eqn. 1. Furthermore, the slope of the line varies with melt composition. These observations imply that ΔE_i is nonzero (i.e., Eqn. 3 should be applied). Q_i can be expressed as a weak function of Z_i^2/r, whereas the activation energy can be modelled better as a function of both M/O and Z_i^2/r:

$$\log\left(\frac{D_i\eta}{T}\right) = -12.4 + 0.245\frac{Z_i^2}{r} + \frac{\left(\frac{Z_i^2}{r} - 12.42\right)(1620\ \mathrm{M/O} - 913)}{T}. \quad (8)$$

The χ^2 statistic for Eqn. 8 when it is applied to the published data set is 0.51 ($n = 253$). Units are the same as for Eqn. 7. The quality of the fit is shown in Figure 7, a comparison of estimated and measured values of $\log(D_i)$ for the entire screened data set. Once again, consistent with the assumptions behind the calculation of χ^2, 90% of the data plots within 0.6 log units of the correlation line (i.e., 2 standard deviations), over a range in diffusivities spanning 10 decades from 10^{-5} to 10^{-15} $\mathrm{cm^2s^{-1}}$.

Eqn. 8 can be used to predict the diffusivity of any IFSE in any magmatic silicate melt at any temperature over the range of conditions under which viscosity is approximately Arrhenian. These conditions obtain in most natural silicate magmas near to or above their liquidus temperatures, and in most felsic compositions even under conditions of strong undercooling during eruption (e.g., Neuville et al., 1993). Diffusivities in fragile basaltic and andesitic melts at temperatures several hundred

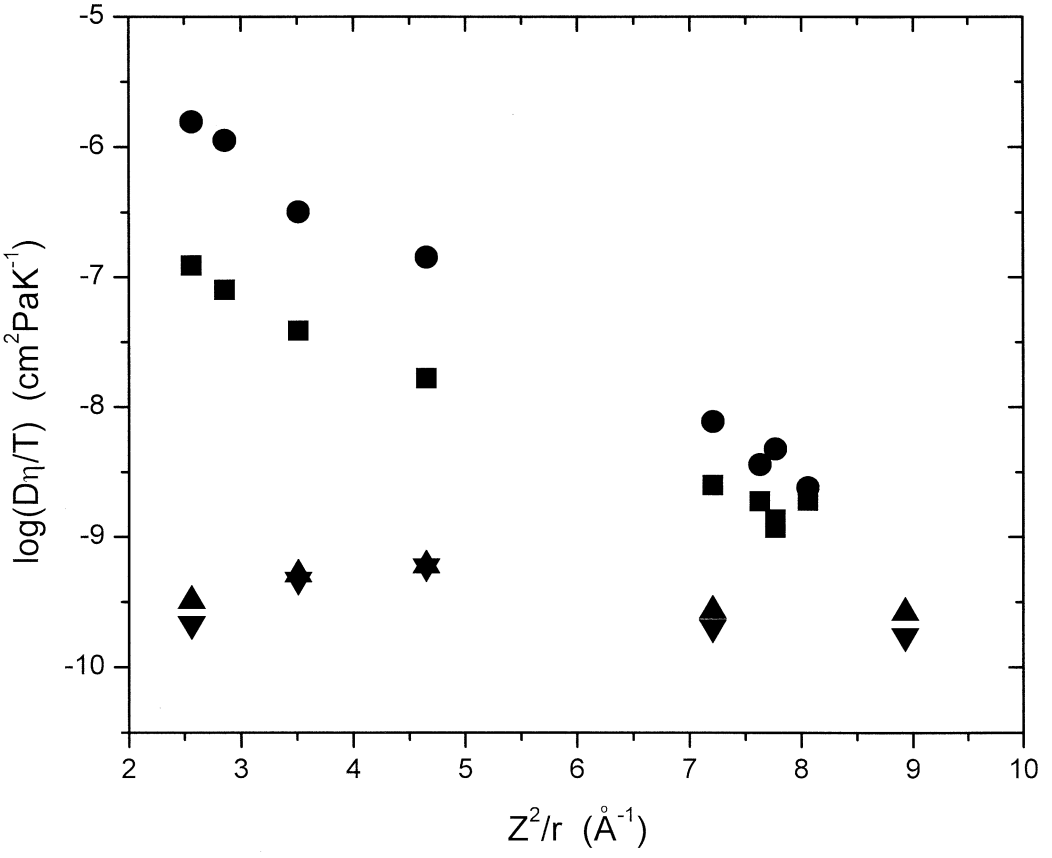

Fig. 6. Log($D_i\eta/T$) vs Z_i^2/r for selected IFSE. Symbols: squares – haplogranite 1400 °C; circles – haplogranite 1137 °C; up triangles – haplobasalt 1400 °C; down triangles – haplobasalt 1500 °C. Data sources: references 13 and 19 in Table 1.

degrees below their liquidus temperatures may depart substantially from values predicted by Eqn. 8.

4.5. Alkali Elements

The values of log($D_i\eta/T$) are plotted against reciprocal temperature for Na in several melts in Figure 8. Log($D_{Na}\eta/T$) is a strong function of reciprocal temperature, so Eqn. 3 is clearly inadequate to account for the data. There is also a noticeable nonlinearity in the data for Na diffusivity in An_{50} and An_{70} plagioclase melts. This nonlinearity is a direct consequence of the non-Arrhenian nature of the viscosity of plagioclase melts. The Arrhenian nature of the diffusivities themselves appears in Figure 9a, where they are plotted against reciprocal temperature. Eqn. 3 was proposed as a way of treating possibly non-Arrhenian data with an Arrhenian model; application of this equation to transform data with an Arrhenian temperature dependence into a non-Arrhenian form would obviously be absurd, so Eqn. 3 is rejected for alkali elements. Furthermore, D_{Na} measured in a very wide range of geological materials (basalt through rhyolite) at high temperatures are subequal as shown in Figure 9a whereas the introduction of the term log($D_{Na}\eta/T$) merely causes these data to separate—note the change in scale between Figures 8 and 9a. Eqn. 6 would thus appear to be the best starting point for an attempt to fit a model to the data.

Since both viscosity and diffusivity show approximately Arrhenian temperature dependence, they will both vary with temperature, and therefore one will seem to vary as an Arrhenian function of the other, but as Figures 8 and 9a show, Na diffusivities in several melts with extremely different viscosities at 1400°C are all subequal—the viscosity is evidently not exerting a controlling influence on diffusivity. A similar pattern was documented by Roselieb and Jambon (1997; Fig. 4), who showed that diffusivities of each alkali cation at a given temperature do not change greatly over the viscosity range represented by the transition from pure liquid silica through jadeite to albite.

Figure 9b shows log(D_{Cs}) in melts with compositions ranging from basaltic to rhyolitic, with water contents of up to 3.7 wt.% and added Na_2O of up to 20 wt.%. Comparison of Figures 9a and 9b indicates that the data for individual melt compositions appear to be Arrhenian over the range of observations, consistent with the form of Eqn. 6 (recall that all data are above T_g). The activation energy of diffusion (i.e., the slope of the trend through the data) decreases with the addition of alkalis or water (decrease in Al/[Na + K + H]), with concomitant decreases in the preexponential factor (intercept with the log[D_i] axis).

Using Jambon's (1982) Arrhenius parameters I have plotted the diffusivities of Li, Na, K, Rb, and Cs in obsidian melt at 600 and 800°C vs. field strength Z_i^2/r in Figure 10. There is a very

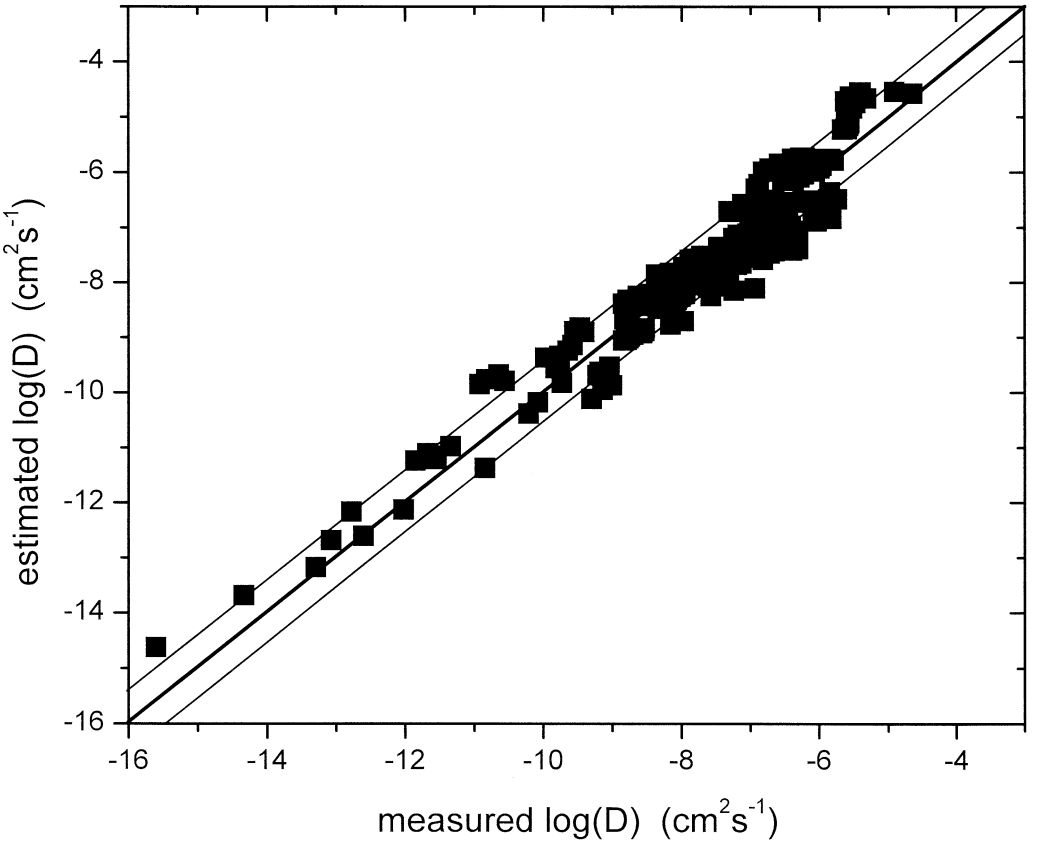

Fig. 7. Comparison of measured and estimated IFSE diffusivities. All of the data set is shown. The bold diagonal line indicates equivalence of measurement and model; fine diagonal lines indicate plus or minus 0.6 log units (two standard deviations). Data sources: references 2, 4, 6, 7, 9, 10, 11, 13, 15, 18, 19.

strong curvature in the isothermal diffusivities, which precludes the use of a linear dependence of $\log(D_i)$ on Z_i^2/r as a means of interpolating or extrapolating from Na and Cs. The curvature has been noted before by Jambon and coworkers, and is also present in plots of activation energy vs. field strength. A similar curvature has been described in both D^i and activation energies for noble gas diffusion (see references in Roselieb and Jambon, 1997). They explain this observation by suggesting that the diffusivities and activation energies depend on the difference between cation radii and a critical radius called the doorway radius. Cations with radius equal to the doorway radius can jump from one potential energy well to another with the greatest of ease, whereas both larger and smaller cations suffer greater hindrance from the network-forming tetrahedra and show higher activation energies and lower D_i. The curvature is removed by employing the parameter $(r_i - d)^2$, where r_i is cation radius and d is the doorway radius.

Figure 11 shows the same data as in Figure 10, plotted vs. $(r_i - d)^2$ for a value of d of 0.103 nm. The dependence is now linear, and the dependence of $\log(D_i)$ on $(r_i - d)^2$ is expected to be quite generally applicable to alkali cations in a variety of melts. The dependences of $\log(D_i)$ on $(r_i - d)^2$, Al/(Na + K + H), and M/O implied by Figures 10 and 11 are expressed in the following equation, with χ^2 equal to 0.44 ($n = 185$):

$$\log(D_i) = -3.02 + (18.5(r_i - 1.03)^2 + 2.88)\mathrm{M/O} - \frac{1}{\mathrm{T}}(538\ \mathrm{A1/(Na + K + H)} + 11910(r_i - 1.03)^2 + 3029). \quad (9)$$

Figure 12a shows all of the data for Na that were plotted in Figures 8 and 9a, compared with the model values. All of the variation in the natural melts is accounted for, and the model continues to work in plagioclase melts with up to 70% An (Al/[Na + K + H] ~ 5). The D_{Na} measured in the most anorthitic melt is not reproduced by the model, due primarily to a departure of activation energy from a linear dependence on Al/(Na + K + H) at the highest values (~19 for An_{90}). Since natural silicate melts almost invariably have Al/(Na + K + H) ratios considerably less than 5, the failure of the model at these very high values of Al/(Na + K + H) is acceptable given its evident success for all other compositions. Figure 12b shows the fit of the model to the data for Cs, even in the very strongly peralkaline melt HPG8 + 20Na_2O (Mungall et al., 1999). Figure 12c shows the remainder of the results, including all published data for Li, K, and Rb. There is a single outlier in this plot, representing the diffusivity of Rb in a diopside melt. The ratio Al/(Na + K + H) is rather meaningless, though nominally equal to 1 in melts contain-

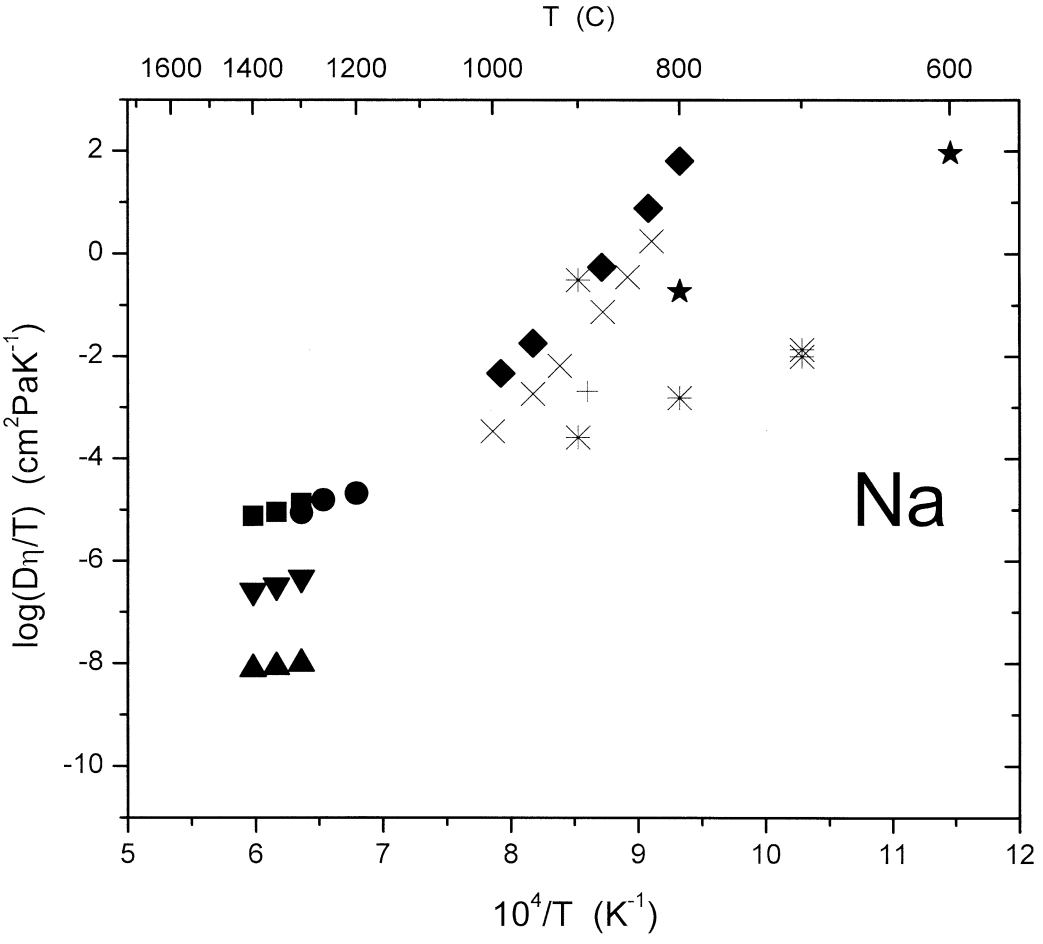

Fig. 8. Log($D_i\eta/T$) vs $10^4/T$ for selected Na data. Symbols: square – pitchstone; circle – pantellerite; up triangle – basalt; down triangle – andesite; diamond – An_{50} plagioclase; x – An_{70} plagioclase; cross – An_{90} plagioclase; asterisk – Lake County obsidian; star – Icelandic obsidian. Note the distinct curvature of the trends for plagioclase. Data sources: references 5, 6, 7, 9, 11 in Table 1.

ing neither alkalis nor alumina, and the resulting point is about 1 log unit off of the measured value. Since natural silicate melts all contain some Al and alkalis, this condition will not occur in natural silicate magmas.

5. DISCUSSION

5.1. Effects of Melt Polymerization

The degree of melt polymerization affects both HFSE and IFSE diffusion, as expressed through the terms involving M/O in Eqn. 7, 8, and 9. The control exercised by field strength on cation mobility is very strong in highly polymerized rhyolitic melts but diminishes to insignificance in the most depolymerized basaltic liquids. It is not surprising that network-modifying cations with high field strength will form tighter links between polymer chains, leading to lower frequency factors and higher activation energies for diffusion than are observed for more weakly bonded low–field strength cations. In depolymerized melts the melt structure will be dominated by the weak network-modifying cation bridges with T-O-M-O-T structures. In this case the melt will be more like a molecular liquid without long-range polymeric structures, and in the absence of a relatively immobile network to which they can become attached, all cations will tend toward similar mobilities. The result would be consistent with the observation that in depolymerized melts rich in network modifiers (e.g., haplobasalt, CAS) all IFSE and HFSE have similar diffusivities close to that predicted by the Eyring equation. Whereas LaTourette et al. (1996) sought explanations for the variations in diffusivity among cations in their haplobasalt liquid, I would draw attention to the fact that compared to the range of diffusivities observed in other melts, their diffusivities are all subequal.

5.2. Mobility of Alkalis

If alkali diffusivity is decoupled from melt viscosity then the diffusive mechanism must not involve net reorganizations of the structure of the melt. This can occur if the mechanism permitting alkali diffusion above T_g involves the network but leaves the network configuration unchanged after it is complete. If the network configuration is not changed after the diffusive step then the size of the rearranging melt region will not be dependent on the configurational entropy of the melt, permitting decoupling of diffusivity from viscosity.

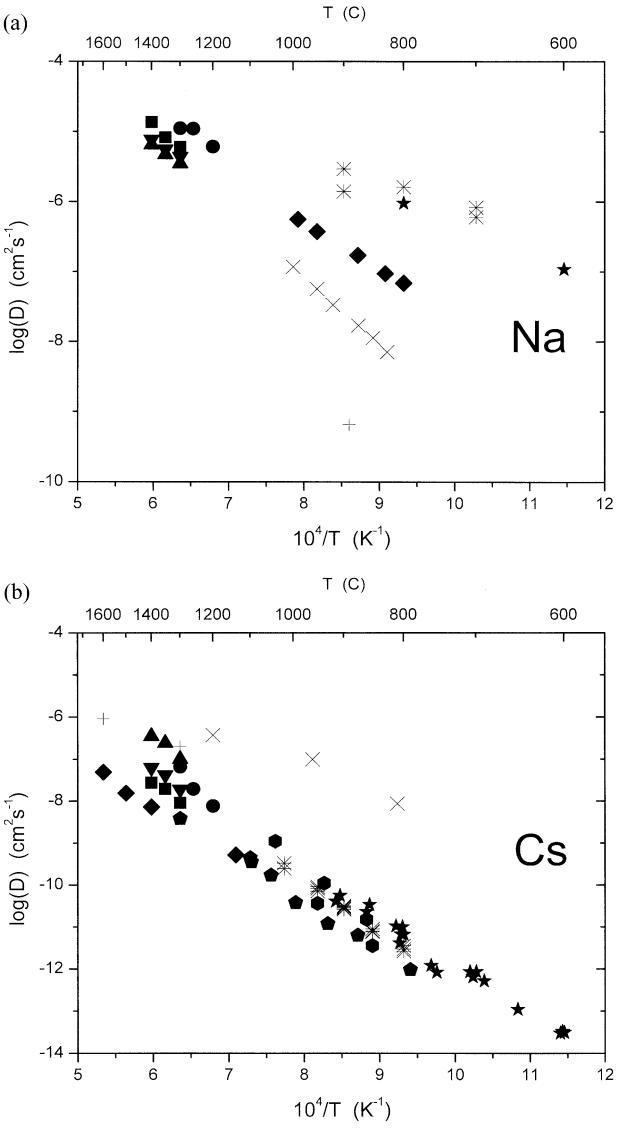

Fig. 9. (a) Log(D_i) vs $10^4/T$ for selected Na data. Symbols as in Figure 8. Note the linear Arrhenian trends for all data. Data sources: references 5, 6, 7, 9, 11 in Table 1. (b) Log(D) vs $10^4/T$ for selected Cs data. Symbols: square – pitchstone; circle – pantellerite; up triangle – basalt; down triangle – andesite; diamond – haplogranite; cross – haplogranite + 3.7 wt% H_2O; x – haplogranite + 20 wt% Na_2O; asterisk – jadeite; hexagon – albite; star – Icelandic obsidian; pentagon – devolatilized Icelandic obsidian. Data sources: references 1, 6, 7, 9, 17, 19 in Table 1.

This may be accomplished through a mechanism similar to that which has been suggested for diffusion of water (Behrens and Nowak 1997), in which pairs of hydroxyl groups break a T-O-T bridge into a nonbridging T-O-H H-O-T configuration. When the two adjacent OH groups recombine they may do so into a different hole on the other side of the temporarily broken T-O-T bond from which they originated. The net result is that an H_2O molecule has jumped from one hole to another through a cooperative motion of two paired OH groups.

I propose a similar mechanism for alkali diffusion; the following discussion refers to Na pairs but could equally well apply to any pair of monovalent cations. In this scenario the rapid diffusion of Na_2O would depend on the presence of paired T-O-Na Na-O-T groups. Because of their very large size compared with a proton, the Na ions would be unable to form Na_2O molecules, but would also be able to attack simultaneously a bridging oxygen in the margins of the hole they occupy in the melt structure. In this way one ONa^- group and one Na^+ ion could jump together from the original T-O-Na Na-O-T group to leave behind a reformed T-O-T bridge, and transform the attacked T-O-T bridge into a new T-O-Na Na-O-T group. At very low alkali contents the simultaneous attack by adjacent T-O-Na Na-O-T groups to form the activated complex for diffusion would be hindered since most O-Na groups would be isolated from one another, accounting for the extreme decrease in Na diffusion in the most Na-poor plagioclase melts (Figs. 9a and 10a), parallelling the extreme decrease in water diffusivity at low water contents (e.g., Zhang et al.,

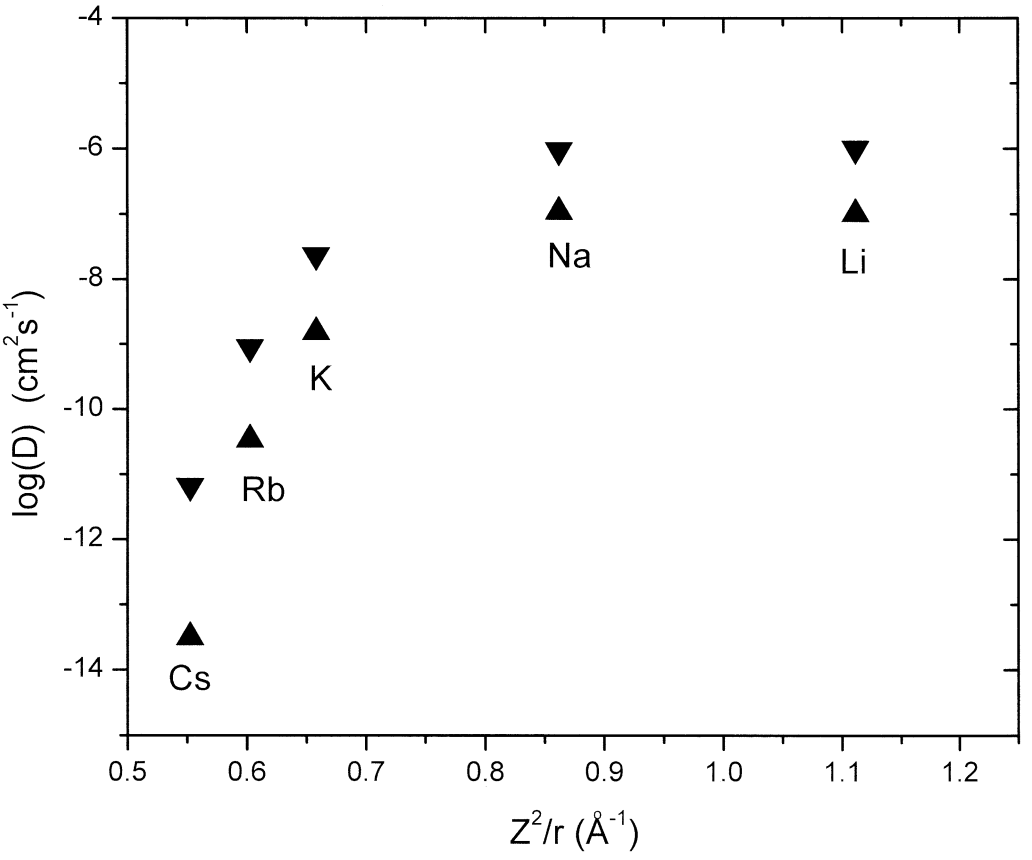

Fig. 10. Log(D_i) vs Z_i^2/r for alkali elements in obsidian melt. Symbols: up triangles – measurements at 600 °C; down triangles – measurements at 800 °C. Note the strong curvature of the isothermal trends. Interpolated from references 1, 3 in Table 1.

1991). The proposed mechanism satisfies the requirement that it involve the network but leave its topology unchanged after a Na_2O group has passed by a point in the melt. Below T_g Na may diffuse by a series of exchanges with other alkali cations, having no interaction with the network (see also Caillot et al., 1994, for discussion of electrical charge–carrying diffusion of alkalis in glasses and melts).

The proposed mechanism is consistent with the observed importance of the ratio Al/(Na + K + H), since the proportion of alkali cations free to diffuse by the proposed mechanism will be diminished by the amount of alkalis required for local charge balance around tetrahedrally coordinated Al^{3+} cations. The requirement that a pair of alkali cations participate together in the diffusive step is also consistent with the observation that larger cations are much less mobile than smaller ones, since pairs of large cations would fit together into the hole much less easily than would small ones. In a given diffusive step, any two alkali cations could form the pair; it would not be necessary for both to be cations of the same element.

5.3. Mobility of Silica and Alumina

The mechanism proposed above for alkali diffusion must be reconciled with the observation that chemical diffusion of Na as a major element in haplogranitic melts can proceed by an exchange with SiO_2 alone (Mungall et al., 1998), leading to SiO_2 and Na_2O concentration profiles of equal length. This observation requires that SiO_2 be just as mobile within the melt as are the alkalis when large chemical potential gradients are present, despite the fact that tracer diffusivity of Na exceeds that of Si by several orders of magnitude.

In an earlier study Mungall et al. (1998) echoed previous suggestions that Si-O-Al bridges would be much stronger than Si-O-Si bridges (e.g., Chakraborty et al., 1995). The reason for this might be found in the description of alkali diffusion above. If the breaking of a T-O-T bridge is facilitated by the presence of paired MO^- groups then one would expect Si-O-Si bridges to participate easily in the process. On the other hand, in the neighborhood of each Si-O-Al bridge there must be an alkali or cation to provide local charge balance. This charge-balancing cation cannot participate in the pair-wise diffusive mechanism because to do so it would have to depart from the alumina tetrahedron, leaving a local charge imbalance. Notwithstanding its inability to participate in the diffusive process, this charge-balancing cation will still take up space in the hole adjacent to the Si-O-Al bridge, requiring three alkali cations to share the restricted space between adjacent polymeric network segments.

The preceding argument indicates that alumina tetrahedra will be effectively barred from participating in the pair-wise alkali diffusive mechanism in polymerized melts due to steric

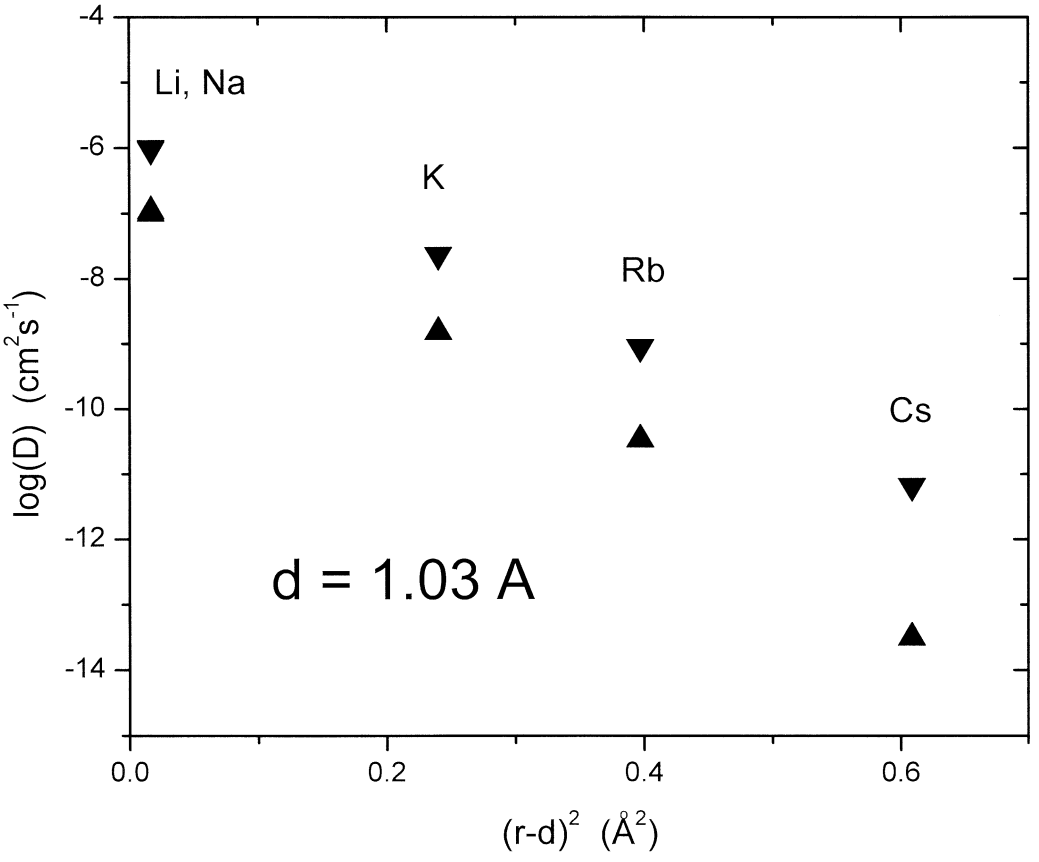

Fig. 11. Log(D_i) vs $(r_i\text{-}d)^2$ for alkali elements in obsidian melt. Data and symbols as in Figure 10. Note the linearity of the isothermal trends. Interpolated from references 1, 3 in Table 1.

hindrance. The actual bond energy required to break Si-O-Al bridges may be similar to that required to break Si-O-Si bridges, but the steric hindrance will result in a much smaller frequency. Thus on an Arrhenian plot the Si-Na exchange will show similar activation energy to the Si-Al exchange, but a much higher intercept, as is observed (Mungall et al., 1998). On the other hand, silica tetrahedra not adjacent to alumina tetrahedra will be capable of being snipped off by the pair-wise alkali diffusive mechanism on all sides. Since the proposed alkali diffusive mechanism directly involves Si-O-Si bridges, the motion of Na will be complemented by a reverse motion of Si at the same rate. The balanced flux of six-oxygen components $Na_{12}O_6$ against Si_3O_6 used by Mungall et al. (1998) implies that each net movement of SiO_2 in one direction requires the sum of four movements of individual Na_2O pairs in the opposite direction, which is exactly what would be required to break sequentially the four Si-O-Si bridges surrounding an individual silica tetrahedron.

It might appear that the possibility of rapid exchange of $Na_{12}O_6$ for Si_3O_6 but not for Al_4O_6 would require that the tracer diffusivity of Si also be substantially greater than that of Al. However, the mechanism for $Na_{12}O_6$–Si_3O_6 exchange is a mechanism for chemical diffusion that will not operate effectively in the absence of a flux of $Na_{12}O_6$. There is no conceptual problem with a chemical diffusivity for a component that greatly exceeds the tracer diffusivity of one of that component's constituent elements. As discussed by Liang et al. (1997), the elements of the multicomponent diffusion matrix depend in a complex way upon the self (~ tracer) diffusivities not only of the ions themselves but also upon the self-diffusivities and charges of all the other ions present in the melt. Major differences between trace and chemical diffusivities are expected when the chemical diffusivity is that of a major component of a multicomponent system.

The key requirement for rapid interdiffusion of $Na_{12}O_6$ for Si_3O_6 is therefore the presence of a chemical potential gradient of $Na_{12}O_6$. $Na_{12}O_6$ will move down its concentration gradient, pushing Si_3O_6 in the opposite direction as it goes. If there is no gradient in $Na_{12}O_6$ concentration, there is no need for silica to move at all by the pair-wise alkali motion, whereas if there is a gradient and a net flux of pairs of Na_2O in one direction, a counterflux of SiO_2 will necessarily result.

The pair-wise diffusive mechanism envisaged by Behrens and Nowak (1997) for water can thus be extended into a powerful concept that accounts for several apparently paradoxical observations of both tracer and chemical diffusion of the alkali and network-forming cations in silicate melts.

5.4. Effects of Pressure

Tracer diffusivities are known to show significant variations with pressure (e.g., Shimizu and Kushiro, 1991; Mungall and

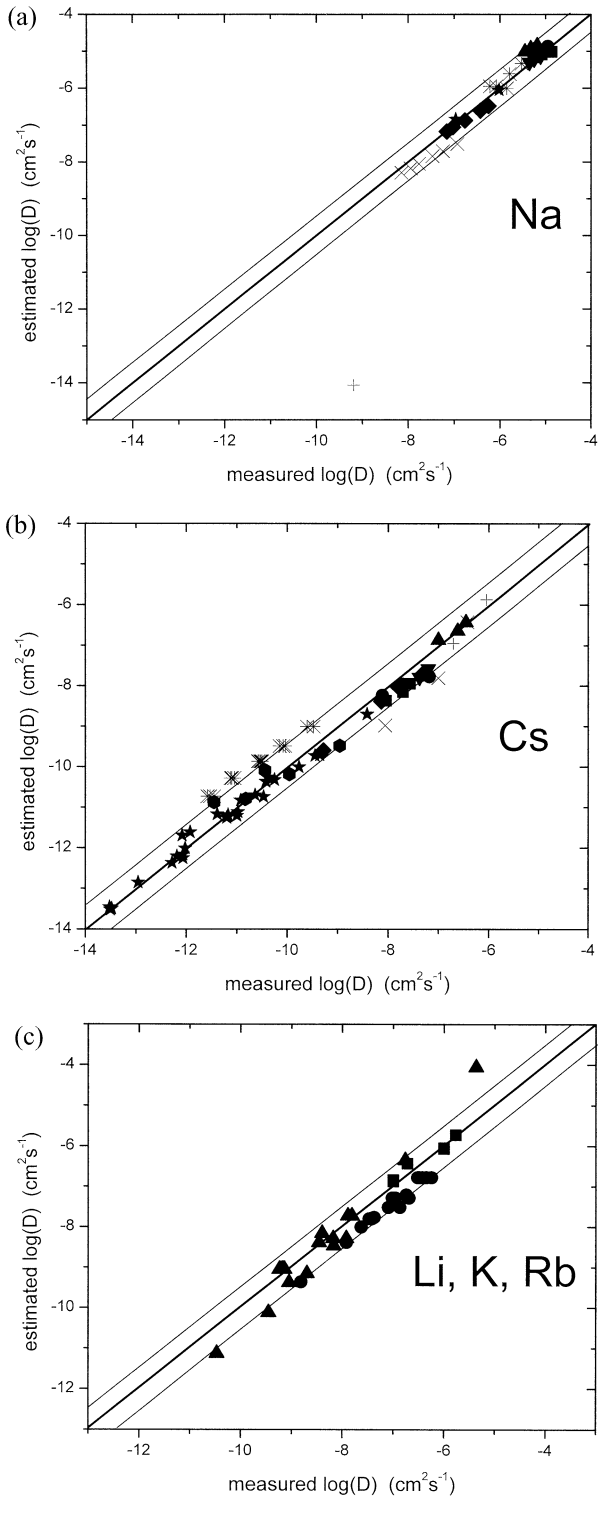

Fig. 12. (a) Comparison of measured and estimated Na diffusivities. Symbols are as in Figure 8. The diagonal line indicates equivalence of measured and model values. See the text for a discussion of the outlier. Data sources: references 5, 6, 7, 9, 11 in Table 1. (b) Comparison of measured and estimated Cs diffusivities. Symbols are as in Figure 9b. The diagonal line indicates equivalence of measured and model values. Data sources: references 1, 6, 7, 9, 17, 19 in Table 1. (c). Comparison of measured and estimated diffusivities of Li, K and Rb. Symbols: square – Li; circle – K; up triangle – Rb. See the text for a discussion of the outlier. Data sources: references 1, 3, 7, 17, 18 in Table 1.

Dingwell, 1997), as are melt viscosities (e.g., Scarfe et al., 1979; Kushiro, 1976), so extrapolation of Eqn. 7, 8, and 9 to pressures typical of the lower crust or upper mantle must take these effects into account. Shimizu and Kushiro (1991) found that the diffusivities of Mg and Ca decreased slightly with increasing pressure whereas the diffusivity of Si showed a substantial increase over the same pressure range. The increase in Si diffusivity corresponds to a reciprocal decrease in melt viscosity, so that recalculation of melt viscosity to account for pressure before use of Eqn. 7 would provide a correct result. On the other hand, the application of a pressure correction to viscosity before using Eqn. 8 to estimate Ca and Mg diffusivities would lead to an error of up to 1 log unit over the pressure range from 0 to 2.5 GPa. Mungall and Dingwell (1997) found that correction of melt viscosities for the effects of pressure allowed the use of the Eyring equation to account for diffusivities of U and Th in a haplogranitic melt at pressures ranging from 0 to 3.5 GPa.

In lieu of a better understanding of the effects of pressure on both diffusion and viscosity of silicate melts, I can only suggest that extrapolation of Eqn. 7 to high pressures be done using viscosities corrected for increases or decreases due to the effects of pressure, whereas Eqn. 8 should be used with uncorrected viscosities. In both cases the maximum error introduced by pressure effects is unlikely to exceed 1 log unit over the pressure range from 0 to 4 GPa.

6. CONCLUSION

The diffusion of cations in silicate melts can be described in the context of the Adam-Gibbs theory of relaxation processes. Diffusivities of alkalis are fully decoupled from the viscosity of the enclosing melt, indicating that the alkalis can move through the melt without requiring readjustments of the topology of the tetrahedrally coordinated network structure. Diffusion of network-modifying cations with intermediate field strength is inferred to proceed by motions involving local rearrangements of the melt structure and can be described using an expanded version of the Eyring equation from which its simpler, classic form was derived. Network-forming and other high–field strength cations are inferred to diffuse by mechanisms similar to those responsible for viscous stress relaxation, and their diffusivities are accounted for by the classic Eyring equation with an additional term for degree of melt polymerization.

The empirical expressions presented here should be useful for the estimation of tracer diffusivities of all cations to which a charge and radius can be assigned in all natural magmatic silicate melts with the possible exceptions of strongly undercooled (i.e., hundreds of degrees Celsius) basaltic liquids. The predictions should be accurate within 1 log unit under all conditions near to the liquidus of any magmatic silicate melt, and in general 90% of estimations are expected to be accurate to within 0.6 log unit. The effects of pressure on diffusivity are implicitly included in the empirical expressions through the pressure dependence of viscosity, so that the results of this study should be applicable throughout the range of conditions at which silicate magmas exist in the Earth.

Further experimental studies should confirm the broad applicability of the empirical models presented here while highlighting the details of their shortcomings. There is no substitute

for careful measurement of transport properties, and it should be evident that the predictions of the models will never be of as high quality as the majority of the data on which they are based. My aim has been to elucidate the underlying processes, and to provide a means of estimation where data are absent and interpolation between well-constrained values is not straightforward.

Acknowledgments—This manuscript has benefitted greatly from the comments of four anonymous reviewers. Special thanks are due to E. Nakamura and I. Kushiro for sharing data before publication, and to E. B. Watson and J. Brenan for helpful discussions of β track methods.

Associate editor: M. S. Ghiorso

REFERENCES

Adam G. and Gibbs J. H. (1965) On the temperature dependence of cooperative relaxation properties in glass-forming liquids. *J. Chem. Phys.* **43,** 139–146.

Baker D. R. (1990) Chemical interdiffusion of dacite and rhyolite: Anhydrous measurements at 1 atm and 10 kbar, application of transition state theory, and diffusion in zoned magma chambers. *Contrib. Mineral. Petrol.* **104,** 407–423.

Baker D. R. (1992a) Estimation of diffusion coefficients during interdiffusion of geological melts: Application of transition state theory. *Chem. Geol.* **98,** 11–21.

Baker D. R. (1992b) Tracer diffusion of network formers and multicomponent diffusion in dacitic and rhyolitic melts. *Geochim. Cosmochim. Acta* **56,** 617–631.

Behrens H. (1992) Na and Ca tracer diffusion in plagioclase glasses and supercooled melts. *Chem. Geol.* **96,** 267–275.

Behrens H. and Nowak M. (1997) The mechanisms of water diffusion in polymerized silicate melts. *Contrib. Mineral. Petrol.* **126,** 377–385.

Bottinga Y. (1994) Configurational entropy and the non-Newtonian rheology of homogenous silicate liquids. *Phys. Rev. B.* **49,** 95–99.

Bottinga Y. and Weill D. F. (1972) The viscosity of magmatic silicate liquids: A model for calculation. *Am. J. Sci.* **272,** 438–475.

Bottinga Y. and Richet P. (1995) Silicate melts: The "anomalous" pressure dependence of the viscosity. *Geochim. Cosmochim. Acta* **59,** 2725–2731.

Caillot E., Duclot M. J., Souquet J. L., Levy M., Baucke F. G. K., and Werner R. D. (1994) A unified model for ionic transport in alkali disilicates below and above the glass transition. *Phys. Chem. Glasses* **35,** 22–27.

Chakraborty S. (1995) Diffusion in silicate melts. *Min. Soc. Am. Rev. Mineral.* **32,** 411–504.

Colson R. O., Keedy C. R., and Haskin L. A. (1995) Diffusion and activity of NiO in CaO-MgO-Al_2O_3-SiO_2 melts considering effects of $a_{O^{2-}}$ and $\gamma_{Ni^{2+}}$. *Geochim. Cosmochim. Acta* **59,** 909–925.

Dingwell D. B. (1990) Effects of structural relaxation in cationic tracer diffusion in silicate melts. *Chem. Geol.* **82,** 209–216.

Einstein A. (1905) Über die von der molekularkinetischen theorie der Wärme geforderte Bewegung von in ruhenden Flüssigkeiten suspendierten Teilchen. *Ann. D. Phys.* **17,** 549.

Ganguly J., Bhattacharya R. N., and Chakraborty S. (1988) Convolution effect in the determination of compositional profiles and diffusion coefficients by microprobe step scans. *Am. Mineral.* **73,** 901–909.

Ghiorso M. S. (1987) Chemical mass transfer in magmatic processes III. Crystal growth, chemical diffusion and thermal diffusion in multicomponent silicate melts. *Contrib. Mineral. Petrol.* **96,** 291–313.

Glasstone S., Laidler K. J., and Eyring H. (1941) *The Theory of Rate Processes*. McGraw-Hill, New York.

Harrison T. M. and Watson E. B. (1983) Kinetics of zircon dissolution and zirconium diffusion in granitic melts of variable water content. *Contrib. Mineral. Petrol.* **84,** 66–72.

Henderson P., Nolan J., Cunningham G. C., and Lowry R. K. (1985) Structural controls and mechanisms of diffusion in natural silicate melts. *Contrib. Mineral. Petrol.* **89,** 263–272.

Hess K.-U. and Dingwell D. B. (1996) Viscosities of hydrous leucogranitic melts: A non-Arrhenian model. *Am. Mineral.* **81,** 1297–1300.

Hess K.-U., Dingwell D. B., and Webb S. L. (1995) The influence of excess alkalis on the viscosity of a haplogranitic melt. *Am. Mineral.* **80,** 297–304.

Hofmann A. W. (1980) Diffusion in natural silicate melts: A critical review. In *Physics of Magmatic Processes* (ed. R. B. Hargraves), pp. 385–417. Princeton University Press, Princeton, NJ.

Hofmann A. W. and Magaritz M. (1977) Diffusion of Ca, Sr, Ba and Co in a basalt melt: Implications for the geochemistry of the mantle. *J. Geophys. Res.* **82,** 5432–5440.

Hummel W. and Arndt J. (1985) Variation of viscosity with temperature and composition in the plagioclase system. *Contrib. Mineral. Petrol.* **90,** 83–92.

International Commission on Radiation Units and Measurements (1984) *International Commission on Radiation Units and Measurements (ICRU) Report 37: Stopping Powers for Electrons and Positrons.* ICRU, Bethesda, MD.

Jambon A. (1982) Tracer diffusion in granitic melts: Experimental results for Na, K, Rb, Cs, Ca, Sr, Ba, Ce, Eu to 1300 °C and a model of calculation. *J. Geophys. Res.* **87,** 10797–10810.

Jambon A. and Carron J.-P. (1976) Diffusion of Na, K, Rb and Cs in glasses of albite and orthoclase composition. *Geochim. Cosmochim. Acta* **40,** 897–903.

Jambon A. and Semet M. P. (1978) Lithium diffusion in silicate glasses of albite, orthoclase, and obsidian composition: An ion-microprobe determination. *Earth Planet. Sci. Lett.* **37,** 445–450.

Kincs J. and Martin S.W. (1996) Non-Arrhenius conductivity in glass: Mobility and conductivity saturation effects. *Phys. Rev. Lett.* **76,** 70–73.

Kuiken G. D. C. (1994) *Thermodynamics of Irreversible Processes: Applications to Diffusion and Rheology*. John Wiley, New York.

Kushiro I. (1976) Changes in viscosity and structure of melt of $NaAlSi_2O_6$ composition at high pressures. *J. Geophys. Res.* **81,** 6347–6350.

LaTourette T., Wasserburg G. J., and Fahey A. J. (1996) Self diffusion of Mg, Ca, Ba, Nd, Yb, Ti, Zr, and U in haplobasaltic melt. *Geochim. Cosmochim. Acta* **60,** 1329–1340.

Lesher C. E. (1990) Decoupling of chemical and isotopic exchange during magma mixing. *Nature* **344,** 235–237.

Lesher C. E. (1994) Kinetics of Sr and Nd exchange in silicate liquids: Theory, experiments and applications to uphill diffusion, isotopic equilibration, and irreversible mixing of magmas. *J. Geophys. Res.* **99,** 9585–9604.

Lesher C. E., Hervig R. L., and Tinker D. (1996) Self diffusion of network formers (silicon and oxygen) in naturally occurring basaltic liquid. *Geochim. Cosmochim. Acta* **60,** 405–413.

Liang Y., Richter F. M., Davis A. M., and Watson E. B. (1996) Diffusion in silicate melts: I. Self diffusion in CaO-Al_2O_3-SiO_2 at 1500 °C and 1 GPa. *Geochim. Cosmochim. Acta* **60,** 4353–4367.

Liang Y., Richter F. M., and Chamberlain L. (1997) Diffusion in silicate melts: III. Empirical models for multicomponent diffusion. *Geochim. Cosmochim. Acta* **61,** 5295–5312.

Lowry R. K., Henderson P. and Nolan J. (1982) Tracer diffusion of some alkali, alkaline-earth and transition element ions in a basaltic and and andesitic melt, and the implications concerning melt structure. *Contrib. Mineral. Petrol.* **80,** 254–261.

Magaritz M. and Hofmann A. W. (1978) Diffusion of Sr, Ba and Na in obsidian. *Geochim. Cosmochim. Acta* **42,** 595–605.

Mungall J. E. and Dingwell D. B. (1997) Actinide diffusion in a haplogranitic melt: Effects of temperature, water content and pressure. *Geochim. Cosmochim Acta* **61,** 2237–2246.

Mungall J. E., Romano C., and Dingwell D. B. (1998) Multicomponent diffusion in the molten system K_2O-Na_2O-Al_2O_3-SiO_2-H_2O. *Am. Mineral.* **83,** 685–699.

Mungall J. E., Dingwell, D. B., and Chaussidon M. (1999) Chemical diffusivities of 18 trace elements in granitoid melts. *Geochim. Cosmochim. Acta* **63,** 2599–2610.

Mysen B. O. and Seitz M. G. (1974) Trace element partitioning determined by beta track mapping: An experimental study using carbon and samarium as examples. *J. Geophys. Res.* **80,** 2627–2635.

Nakamura E. and Kushiro I. (1998) Trace element diffusion in jadeite and diopside melts at high pressures and its geochemical implications. *Geochim. Cosmochim. Acta* **62,** 3151–3160.

Neuville D. R., Courtial P., Dingwell D. B., and Richet P. (1993) Thermodynamic and rheological properties of rhyolite and andesite melts. *Contrib. Mineral. Petrol.* **113,** 572–581.

Press W. H., Teukolsky S. A., Vetterling W. T., and Flannery B. P. (1992) *Numerical Recipes in FORTRAN: The Art of Scientific Computing*, 2nd ed. Cambridge University Press, Cambridge, UK.

Richet P. (1984) Viscosity and configurational entropy of silicate melts. *Geochim. Cosmochim. Acta* **48,** 471–483.

Richter F. M., Liang Y., and Davis A. M. (1999) Isotope fractionation by diffusion in molten oxides. *Geochim. Cosmochim. Acta* **63,** 2853–2861.

Roselieb K. and Jambon A. (1997) Tracer diffusion of potassium, rubidium, and cesium in a supercooled jadeite melt. *Geochim. Cosmochim. Acta* **61,** 3101–3110.

Scarfe C. M., Mysen B. O., and Virgo D. (1979) Pressure dependence of the viscosity of silicate melts. In *Magmatic Processes: Physicochemical Principles* (ed. B. O. Mysen), *Geochem. Soc. Spec. Publ.* **1,** pp. 59–67.

Shannon R. D. (1976) Revised effective ionic radii and systematic studies of interatomic distances in halides and chalcogenides. *Acta Cryst. A.* **32,** 751–767.

Shaw H. R. (1972) Viscosities of magmatic silicate liquids: an empirical method of prediction. *Am. J. Sci.* **272,** 870–893.

Shimizu N. and Kushiro I. (1991) The mobility of Mg, Ca, and Si in diopside-jadeite liquids at high pressures. In *Physical Chemistry of Magmas Advances in Physical Geochemistry 9* (eds. L. L. Perchuk and I. Kushiro), pp. 192–212. Springer-Verlag, New York.

Tingle T. N. (1987) An evaluation of the carbon-14 beta track technique: Implications for solubilities and partitioning coefficients determined by beta track mapping. *Geochim. Cosmochim Acta* **51,** 2479–2487.

Urbain G., Bottinga Y., and Richet P. (1982) Viscosity of liquid silica, silicates and aluminosilicates. *Geochim. Cosmochim. Acta* **46,** 1061–1072.

Watson E. B. (1979) Calcium diffusion in a simple silicate melt to 30 kbar. *Geochim. Cosmochim. Acta* **43,** 313–322.

Watson E. B. (1981) Diffusion in magmas at depth in the Earth: The effects of pressure and dissolved H_2O. *Earth Planet. Sci. Lett.* **52,** 291–301.

Zhang Y., Stolper E. M., and Wasserburg G. J. (1991) Diffusion of water in rhyolitic glasses. *Geochim. Cosmochim. Acta* **55,** 441–456.

APPENDIX

A.1. Stokes-Einstein Equation

The diffusion of colloidal particles by Brownian motion in water was discussed by Einstein (1905). He combined a statistical description of particle distributions in an externally applied potential field with the description of Stokes flow around a hard sphere in a viscous suspending fluid to arrive at the simple expression

$$D_i = \frac{\kappa T}{6\pi\eta r_i}. \tag{A1}$$

The diffusivity D_i is exactly analogous to a tracer diffusivity. T is the absolute temperature, κ is Boltzman's constant, η is the viscosity of the suspending fluid, and r_i is the radius of the colloidal particle. Because of its derivation in continuum mechanics, this equation is not applicable to cationic diffusion, because the ion cannot be considered to be diffusing through a continuum of fixed viscosity; it is mentioned here because of its frequent misapplication to tracer diffusion in silicate melts.

A.2. Eyring Equation

Eyring and coworkers developed a description of diffusion and viscosity using transition state theory during the 1930s that was succinctly described by Glasstone et al. (1941). They derived a series of equations showing that there is a fundamental identity of diffusion and stress relaxation in melts. Combining their Eqn. 14, 23, 31, and 155 leads to the following general relation:

$$\frac{D_i\eta}{T} = \frac{\lambda_i^2\kappa}{\lambda_\nu^3}\left(\frac{\nu_\nu}{\nu_i}\right)^{1/3}\left(\frac{m_\nu}{m_i}\right)^{1/2}\exp\left\{\frac{\varepsilon_\nu - \varepsilon_i}{\kappa T}\right\}. \tag{A2}$$

In equation A3 the quantities subscripted *i* refer to the properties of a solute particle undergoing a diffusive motion whereas those subscripted *v* refer to the properties of a melt species whose motion permits reorganization of the melt structure and thereby relaxes an imposed stress. *v* is the free volume surrounding a melt species, *m* is the mass of a melt species, ε is the activation energy for motion a solute particle, λ is its radius, κ is Boltzmann's constant, and T is absolute temperature.

If the melt under consideration is a one-component melt, then the quantities subscripted *v* and *i* will be identical, and Eqn. A2 reduces to the familiar form below:

$$D_i = \frac{\kappa T}{\eta\lambda}, \tag{A3}$$

generally known as the Eyring equation, and D_i becomes the self-diffusivity of the single component present. In a multicomponent melt, the terms subscripted *v* and *i* will probably not be identical, the classic form of the Eyring equation will not accurately describe the relation between viscosity and diffusion, and Eqn. A2 should be used instead.

A.3. Adam-Gibbs Theory

Adam and Gibbs (1965) considered the temperature dependence of viscous stress relaxation, based on thermodynamic arguments. Their equation for viscous relaxation time can be combined with the Maxwell relation (e.g., Dingwell, 1990) and expressed as follows:

$$\eta = A_\nu G\exp\left\{\frac{s_c'\Delta\mu_\nu}{\kappa T S_c}\right\}, \tag{A4}$$

where η is the zero-frequency Newtonian viscosity, A_ν is a preexponential constant analogous to that in Eqn. A3, $\Delta\mu_\nu$ is the activation energy for the fundamental movement permitting viscous flow, s'_c is the configurational entropy of the smallest melt volume capable of undergoing a cooperative rearrangements that permit viscous flow, G is the infinite frequency shear modulus of the melt (of the order 10 GPa; cf. Dingwell, 1990) and S_c is the configurational entropy of the melt as a whole. Configurational entropy of glass-forming liquids is a function of temperature that can be inferred directly by a calorimetric measurement cycle from absolute zero through T_g. Eqn. A4 can be used to establish two empirically derived constants equivalent to A_ν' and $s_c\Delta\mu_\nu'/k$ for a given melt composition for which the configurational entropy is calculable, and reproduces actual melt viscosities within experimental error over the entire accessible range of viscosity measurements (e.g., Richet 1984, Neuville et al., 1993). The Adam-Gibbs theory can also be used to account for observations of both shear thinning and pressure dependence of viscosity (Bottinga, 1994; Bottinga and Richet, 1995), and is consequently the best conceptual framework currently available for quantitative descriptions of viscous flow.

The Adam-Gibbs equations describe ionic motions permitting viscous stress relaxation within the melt. These motions equally well can be considered in the context of diffusive relaxation of chemical potential gradients. An equation similar to Eqn. A4 can be written to describe diffusion of each melt component, in which the critical size of the cooperatively rearranging region permitting a diffusive motion and the preexponential frequency factor will be functions of the solute particle's characteristics (e.g., charge, radius):

$$D = \frac{\lambda_i^*}{A_i^*}\exp\left\{\frac{-s_c''\Delta\mu_i}{\kappa T S_c}\right\}, \tag{A5}$$

where λ_i is a characteristic length scale that may be taken as the jump distance, A_i is a constant, s_c'' is the configurational entropy of the melt region that must be rearranged to allow a diffusive jump, $\Delta\mu_i$ is the activation energy of the rearrangement, and k and S_c are as before.

Eqn. A4 and A5 can be combined to arrive at the following relation between melt viscosity and the diffusion of solute species:

$$D\eta = \frac{\lambda_i^2 G A_\nu^*}{A_i^*} \exp\left\{\frac{(s_c'\Delta\mu_\nu - s_c''\Delta\mu_i)}{\kappa T S_c}\right\}. \quad \text{(A6)}$$

In Eqn. A6 the timescales of diffusion and viscous flow are tied to one another through their common dependence on the configurational entropy of the melt. Variations in melt viscosity will lead to concerted variations in the diffusivities of all solute species whose motions depend in some way on the reorganization of the melt structure.

If diffusive jump mechanisms do not involve a net rearrangement of the network, then the size of the cooperatively rearranging region does not depend on temperature, nor does it depend on the mobility of the melt structure. In this case, by analogy to Adam and Gibbs (1965, (their eq 8) Eqn. 8),

$$D = \frac{\lambda_i^2}{A_i} \exp\left\{\frac{-z_i\Delta\mu_i}{\kappa T}\right\}. \quad \text{(A7)}$$

Diffusivity in Eqn. A7 now shows no dependence on the configurational entropy of the melt. As a result of this lack of correlation between configurational entropy and diffusion, Eqn. A7 and A4 cannot be linked in any useful way. Diffusion and viscosity have been completely decoupled, and therefore changes in melt viscosity will have no effect on the diffusivity of solute species whose diffusive motion does not require cooperative rearrangements of the melt structure. Thus the diffusivities of individual melt species whose diffusive motion does not require net rearrangements of the melt structure may be equal in different melts with very different viscosities.

Caillot et al. (1994) proposed a somewhat different approach to modelling the relation between diffusion and viscosity in melts that show non-Arrhenian viscosity variations. They employed a model equation based on free-volume theories of viscous flow, using a VTF-type of formulation. They also suggested that an Adam-Gibbs formulation might be applied, but did not pursue this avenue.

Shimizu and Kushiro (1991) used an approach based on the Adam-Gibbs theory to account for variations in tracer diffusivities in the system diopside-jadeite, demonstrating that configurational entropies could be used to predict compositional dependences of diffusivity as well as viscosity.

In light of the demonstrated superiority of the Adam-Gibbs formulation over VTF-type equations in description of silicate melt viscosities (e.g., Urbain et al., 1982; Richet, 1984; Hummel and Arndt, 1985; Bottinga, 1994; Bottinga et al., 1995), I have adopted the Adam-Gibbs approach.